Research Article

Brain expressed *FKBP5* delineates a therapeutic subtype of severe mental illness

Natalie Matosin[1,2,3]*, Janine Arloth[1,4], Silvia Martinelli[1], Darina Czamara[1], Malosree Maitra[5], Thorhildur Halldorsdottir[6], Cristiana Cruceanu[1], Dominic Kaul[2,3], Nils C. Gassen[1,7], Kathrin Hafner[1], Nikola S Müller[4], Karolina Worf[4], Ghalia Rehawi[1,4], Corina Nagy[5,13], Elizabeth Scarr[8], Ran Tao[9], Andrew E. Jaffe[9], Thomas Arzberger[10,11], Peter Falkai[10], Joel E. Kleinmann[9,12], Daniel R. Weinberger[9,12], Naguib Mechawar[5,13], Andrea Schmitt[10,14], Brian Dean[15], Gustavo Turecki[5,13,16], Thomas M. Hyde[9,12], Elisabeth B. Binder[1,17]*

[1] Department of Translational Research in Psychiatry, Max-Planck Institute of Psychiatry, Munich, Germany
[2] Illawarra Health and Medical Research Institute, Northfields Ave, Wollongong 2522, Australia
[3] Molecular Horizons, School of Chemistry and Molecular Biosciences, Faculty of Science, Medicine and Health, University of Wollongong, Northfields Ave, Wollongong 2522, Australia
[4] Institute of Computational Biology, Helmholtz Zentrum München, Neuherberg 85764, Germany
[5] McGill Group for Suicide Studies, Douglas Mental Health University Institute, Montreal, Quebec, Canada
[6] Department of Psychology, Reykjavik University, Reykjavik, Iceland
[7] Neurohomeostasis Research Group, Institute of Psychiatry, University of Bonn, Clinical Centre, Bonn, Germany
[8] Melbourne Veterinary School, Faculty of Veterinary and Agricultural Sciences, The University of Melbourne, Parkville, Victoria 3010
[9] The Lieber Institute for Brain Development, Johns Hopkins University Medical Campus, Baltimore, MD, USA
[10] Department of Psychiatry and Psychotherapy, University Hospital, Ludwig-Maximilians University Munich, Nussbaumstrasse 7, 80336 Munich, Germany
[11] Centre for Neuropathology and Prion Research, Ludwig-Maximilians University Munich, Nussbaumstrasse 7, 80336 Munich, Germany
[12] Department of Psychiatry and Behavioral Sciences at Johns Hopkins University School of Medicine
[13] Department of Psychiatry, McGill University, Montreal, Quebec, Canada
[14] Laboratory of Neuroscience (LIM27), Institute of Psychiatry, University of Sao Paulo, Rua Dr. Ovidio Pires de Campos 785, 05453-010 São Paulo, Brazil
[15] Molecular Psychiatry Laboratory, Florey Institute for Neuroscience and Mental Health, Parkville, VIC, Australia
[16] Department of Human Genetics, McGill University, Montreal, Quebec, Canada
[17] Department of Psychiatry and Behavioral Sciences, Emory University School of Medicine, Atlanta, USA

*** Correspondence**
Email: nmatosin@uow.edu.au
Email: binder@psych.mpg.de

SUMMARY

Deducing genes capable of classifying biologically-distinct psychiatric subtypes, and their targets for treatment, is a priority approach in psychiatry. *FKBP5* is one such gene with strong evidence of utility to delineate a trans-diagnostic psychiatric subtype. Yet how brain-expressed *FKBP5* is affected in psychiatric disorders in humans is not fully understood and critical for propelling *FKBP5*-targeting treatment development. We performed a large-scale postmortem study (n=895) of *FKBP5* using dorsolateral prefrontal cortex samples derived from individuals with severe psychiatric disorders with a comprehensive battery of bulk/single-cell omics and histological analyses. We observed consistently heightened *FKBP5* mRNA and protein in psychopathology, moderated by genotype and age, and accompanied by DNA methylation changes in key enhancers. These effects were most prominent in superficial-layer pyramidal cells. Heightened *FKBP5* was also differentially associated with downstream pathways according to age, being specifically associated with synaptic transmission in early adulthood, and neuroinflammation and neurodegeneration in later life.

Keywords: FKBP5, FKBP51, psychosis, depression, aging, epigenetics, stress, single-cell, postmortem brain

INTRODUCTION

The approved use of available drugs for specific psychiatric diagnoses – and their prescription to specific patients – are currently not based on biological knowledge of the pathological mechanisms that contribute to an individual's disease presentation. Increased understanding of the genetic and molecular underpinnings of psychiatric disease is critical to facilitate mechanism-based diagnoses of biologically distinct patient subgroups, and the corresponding biological targets for their treatment (Visscher et al., 2017). Yet very few genes have been translated from genetic studies to mechanistic and biomarker levels in various populations; FK 506 Binding Protein 51 kDa (FKBP51) is one of these few. FKBP51 is encoded by the gene *FKBP5* on chromosome 6p21.31, and is an allosteric heat shock protein 90 kDa (HSP90) co-chaperone of the glucocorticoid receptor (GR). FKBP51 is highly responsive to glucocorticoid (cortisol)-mediated stress, and physiologically important for propagating and terminating the stress response (Zannas et al., 2016). Human genetic, epigenetic and animal studies consistently indicate that heightened FKBP51 expression in individuals exposed to early life adversity may contribute to psychiatric disease risk in a subset of patients (Matosin et al., 2018). FKBP51 antagonism is a proposed therapeutic mechanism for this patient subgroup (Matosin et al., 2018).

FKBP5 transcription throughout the body has been shown to naturally increase over the lifespan (Blair et al., 2013; Matosin et al., 2018; Weickert et al., 2015), and this expression over time is likely moderated by several factors including stress and genetic variants. Glucocorticoid-induced *FKBP5* transcription is triggered by activation of glucocorticoid response elements (GREs) located within upstream enhancers and intronic regions of *FKBP5* (Wiechmann et al., 2019). The strength of this induction is moderated by two mechanisms, genetic and epigenetic. Firstly, minor allele carriers of a functional common *FKBP5* haplotype (tagged by the single nucleotide polymorphism [SNP] rs1360780 T allele in intron 2) show exacerbated *FKBP5* induction following stress or glucocorticoid exposure. Secondly, reduced DNA methylation (DNAm) at key *FKBP5* GREs is also associated with higher *FKBP5* mRNA induction (Klengel and Binder, 2015; Klengel et al., 2013). These two mechanisms appear to converge and compound in some individuals: DNAm at *FKBP5* GREs is decreased in individuals who carry the *FKBP5* minor allele haplotype and who have been specifically exposed to early life adversity, a major risk factor for psychiatric disease (Kendler et al., 1999; Kendler et al., 2011). The genetic predisposition combined with exposure to early life adversity thus contributes to combined genetic and epigenetic disinhibition of *FKBP5* transcription in response to stress (Klengel and Binder, 2015; Klengel et al., 2013). This leads to much higher levels of *FKBP5* transcription after each stress exposure in this specific patient subset, hypothesised to cause a dysregulated cellular and systemic stress response that sets these individuals on a trajectory towards psychiatric illness later in life (Figure 1).

The extensive evidence of heightened *FKBP5* expression as a trans-diagnostic risk factor for psychiatric disorders has spurred the development of small-molecule *FKBP5* antagonists as novel therapeutics (Gaali et al., 2015; Matosin et al., 2018). These agents have a promising profile of effects, with preclinical experiments in rodents showing that *FKBP5* antagonists improve stress-coping behaviour and reduce anxiety when given systemically or directly into relevant brain regions such as the amygdala (Gaali et al., 2015; Hartmann et al., 2015). To move development of this drug-class forward, comprehensive characterisation of *FKBP5* directly in a large transdiagnostic brain sample is needed, as this is where psychiatric symptoms primarily manifest and therapeutics are most likely to exert their effects. This includes understanding of brain-expressed *FKBP5* across multiple regulatory levels (genetic variation, DNA methylation, transcript and protein) and its cell-type specificity.

In the largest and most comprehensive study to date, we examined an extensive collection (total N = 895) of human postmortem dorsolateral prefrontal cortex samples (Brodmann area 9; BA9) derived from individuals who lived with schizophrenia, major depression or bipolar disorder and controls. The dorsolateral prefrontal cortex is a brain area that is highly implicated in psychiatric disorders, associated with executive functioning and working memory processes, which are impaired by stress and hallmark symptoms of trans-diagnostic psychopathology (Arnsten, 2009). We used bulk and single-cell omics approaches and advanced histological methods to explore the convergence of *FKBP5* haplotype, transcription, epigenetic regulation, translation, as well as the cell-type- and cortical-layer-specific patterns of expression. We found subtype-based expression differences with divergence at the age of 50, after which we observed marked increases in *FKBP5* expression, particularly in *FKBP5* risk haplotype carriers. We also showed that these effects converge specifically on excitatory pyramidal cells in the superficial cortical layers of BA9, and that heightened *FKBP5* in older subjects likely causes an increased neuroinflammatory and neurodegenerative profile in this patient subgroup. These results support the utility of *FKBP5* as a biomarker for a new, biologically-delineated psychiatric patient subgroup, and the development of FKBP51 antagonists as a treatment option for these patients.

RESULTS

FKBP5 and FKBP51 expression levels are significantly higher in cases compared to controls

To comprehensively understand how expression patterns of *FKBP5* gex and FKBP51 protein are altered in severe psychopathology, we used the largest sample to date to assess *FKBP5* cortical expression differences in cases compared to controls (see Table 1 for explanation of postmortem cohort "Series" and sample sizes; analyses approaches detailed in the methods). Adjusting for age, we observed a striking increase (+28.05%) in *FKBP5* gene expression (gex) in all cases (Series 1: t=3.299, P_{NOM}=0.001043), driven mainly by +39.83% higher *FKBP5* gex in subjects with schizophrenia (t=3.226, P_{NOM}=0.001403) and depression (+23.86%; t=2.478, P_{NOM}=0.01377). In bipolar disorder, the effect size was in the same direction (+4.04%) but did not reach statistical significance likely due to a more limited sample size (t=1.241, P_{NOM}=0.21578; Figure 2a). We replicated this finding in an independent sample (Series 2, n=169, see Table 1), with an increase in *FKBP5* gex between cases vs controls (t=2.463, P_{NOM}=0.0149, +2.5%) and schizophrenia subjects vs controls (t=2.600, P_{NOM}=0.01058, +2.1%) (Figure 2a). FKBP51 protein (Series 2) was also increased in schizophrenia cases vs controls (t=2.247, P_{NOM}=0.0317, +9.74%). As for *FKBP5* gex, FKBP51 protein levels were increased, although not significantly different, between depression and bipolar disorder subjects vs controls (Figure 2a). *FKBP5* and FKBP51 levels in Series 2 were also strongly and positively correlated in all subjects (R=0.507, P_{NOM}=4.57 e-05, Figure 2b). These results together indicate that *FKBP5* and FKBP51 gex and protein levels are increased in psychiatric cases vs controls, with the largest effect sizes noted in schizophrenia subjects.

FKBP5 and FKBP51 expression levels increase with age in controls, with this aging-related increase exacerbated in psychiatric cases

Of note, we observed a strong effect of age on *FKBP5* and FKBP51 consistent with previous reports (Blair et al., 2013; Matosin et al., 2018; Weickert et al., 2015). To further resolve aging effects on *FKBP5* and FKBP51 expression, we firstly characterised the trajectory of *FKBP5* gex over the life-course in healthy control subjects in Series 1 (n=340). Gex inflected in childhood and adolescence and increased consistently through adulthood (20-50 years; R=0.253, P_{NOM}=0.0160) and into older ages (50-96 years; R=0.334, P_{NOM}=0.0097; Figure 2c). The positive association of gex with age in controls in adulthood was also seen in Series 2 (Figure S1b; R=0.61343, P_{NOM}=1.153e-07) and validated with qPCR using two probes targeting total *FKBP5* gex in Series 3 (Probe 1, R=0.460, P_{NOM}=0.024; Probe 2, R=0.449, P_{NOM}=0.028; Figure S1c). FKBP51 total protein expression was also positively correlated with age in adulthood (Series 3; R=0.500, P_{NOM}=0.014; Figure 2d).

We then assessed if the aging trajectory of *FKBP5* gex was heightened in cases vs controls (subjects >14 years). In Series 1, the aging trajectory of *FKBP5* gex was not different for all cases vs controls,

but the gex-aging slope was significantly heightened in schizophrenia subjects vs controls (P_{FDR}=0.0232; Figure 2e). In particular, we noted +29.44% higher *FKBP5* gex in schizophrenia subjects over 50 (P_{NOM}=0.05). The aging trajectory of total *FKBP5* gex in major depressive disorder was not different compared to controls after multiple correction (P_{FDR}=0.076), but gex was heightened in subjects with major depression over 50 (P_{NOM}=0.038, +22.4%). There was no difference between bipolar disorder patients vs controls over 50 (P_{NOM}=0.808). In Series 2, *FKBP5* was also positively and significantly associated with age in both cases (all grouped: R=0.4159, P_{NOM}=9.242e-06 and schizophrenia specifically: R=0.4817, P_{NOM}=3.201e-05) and controls (R=0.61343, P_{NOM}=1.153e-07). When comparing the *FKBP5* gex aging trajectories of cases vs controls, there was a borderline difference overall (P_{NOM}=0.056) and none of the specific diagnoses vs control comparisons reached statistical significance. However, we again observed divergence in the gex and protein aging trajectories in cases (all grouped) compared to controls at approximately 50 years of age (gex: Figure S1b, protein: Figure 2f). These results consistently suggest that *FKBP5* mRNA and FKBP51 protein levels are heightened in older patients with schizophrenia and major depression compared to controls.

Combined effects of aging and *FKBP5* risk genotype increase *FKBP5* expression in psychiatric cases

Previous studies indicate that *FKBP5* gex is differentially induced based on *FKBP5* rs1360780 genotype following stimulation by GR agonists, with minor allele (T) carriers exhibiting the highest levels of *FKBP5* gex after such stimulation (Klengel and Binder, 2013; Menke et al., 2013). We tested for interactive effects of this genotype on *FKBP5* gex and case-status (all cases combined, sample sizes in Supplemental Table 7). We observed main effects of both case-status (B=0.0092, t=2.277, P=0.0233) and the rs1360780 genotype (B=-0.0166, t=-2.401, P=0.0168), but there was no significant interaction of case-status and genotype overall (genotype × case-status: B=0.00699, t=1.264, P=0.2068) on *FKBP5* gex levels. As the lack of a significant interaction effect between case-status and genotype could be due to a diluted effect when cross-comparing all four case-status/genotype groups (i.e., minor and major allele carriers), we also performed a direct comparison of case risk-allele T carriers compared to the other case-status/genotype groups. *FKBP5* gex was heightened in cases carrying the risk T-allele compared to control CC homozygotes (+44.7%, P_{FDR}=0.001195) and control T carriers (+28%, P_{FDR}=0.01104), but there was no difference compared to case CC homozygotes (Figure 3a).

Given the clear divergence of aging trajectories between case-control groups over 50 (Figure 2e/f and 3b) and the observed genotype effects, we further examined *FKBP5* gex between case-and-control genotype groups in subjects 50 to 75 years. In this age group, cases carrying the T allele had the highest level of *FKBP5* gex ($P_{FDR}\leq$0.024, Figure 3b). Although in a modest sample size (n=38 case and 24 control CC homozygotes, 72 case and 66 control T carriers), these findings suggest there are

effects of the *FKBP5* rs1360780 genotype on total *FKBP5* gex over aging, as well as case-status. Overall, these findings indicate convergence of aging and genotype effects on *FKBP5* that contribute to the heightened levels of expression observed in psychopathology.

Case-status, age and increased gene expression associate with lower *FKBP5* DNAm at key enhancer sites

DNAm changes at key enhancer sites can lead to lasting and cumulative changes in gex (Moore et al., 2013). Specifically, *FKBP5* DNAm associates with age in brain (Blair et al., 2013) and peripheral blood (Zannas et al., 2019). We therefore explored whether the observed case-control status, age and genotype-related differences in gex were associated with DNAm changes. We grouped CpGs functionally by (i) genomic position within the *FKBP5* locus, (ii) results of our previous targeted bisulfite sequencing of *FKBP5* DNAm in response to GR activation (Wiechmann et al., 2019) and (iii) functional quantitative chromatin immunoprecipitation experiments (Paakinaho et al., 2010). Using data from the Illumina 450k DNA methylation arrays, the average percentage DNAm of CpGs was assessed for the distal topologically associating domain (TAD), a downstream conserved methylation quantitative trait locus (mQTL), the intron 5 GRE (Wiechmann et al., 2019), the transcription start site (TSS), the proximal enhancer GREs (grouped together as well as analysed as potentially independently functioning CpGs), and the proximal TAD (Supplemental Table 8).

We firstly identified single CpGs/regions where DNAm was associated with gex levels in Series 1 (Supplemental Table 9). A negative correlation between total *FKBP5* gex and DNAm was observed in the downstream conserved region (R=-0.102, P_{NOM}=0.022) and the proximal enhancer (total group: R=-0.1458, P_{NOM}=0.0011); specifically, we observed that lower DNAm in these regions was associated with higher gex (Figure 3c and 3d). Lower DNAm at the proximal enhancer was also observed in cases compared to controls, specifically at the cg25114611 CpG in the proximal enhancer (t=-3.251, P_{FDR}=0.007, -2.94%; Supplemental Table 10). This difference was mainly carried by the schizophrenia group compared to controls (P_{FDR}=0.004, -4.44%; Figure S1d). DNAm was also significantly correlated with age in a number of regions, including a strong negative correlation in the proximal enhancer (total, R=-0.788, P_{NOM}=6.447e-106; Figure 3d and Supplemental Table 11). However, there were no clear genotype effects on DNAm in any of the regions. Together, these results indicate that there is convergence of case-status and age on DNAm levels in the proximal enhancer of *FKBP5*. Specifically, lower DNAm was associated with case-status, age, and higher gene expression. This is in line with the significant negative correlation of DNAm in this enhancer and gex in the total sample.

***FKBP5* and FKBP51 are prominently expressed in superficial-cortex excitatory neurons, and increased in cases compared to controls in these neurons**

We next aimed to gain deeper mechanistic insight into the cell-type contributions of heightened *FKBP5* in the human brain, by assessing *FKBP5* cell-type distribution, cortical-layer specificity and the cell-type specificity of aging effects in the BA9 brain area. Focusing on single-nucleus RNA sequencing (snRNAseq) data from Series 4, we examined differential *FKBP5* gex expression between cell types. Among the 26 delineated cell-type clusters in Series 4 (n=34), *FKBP5* gex was most highly expressed on microglia, astrocytes and excitatory neurons (Figure 4a), and statistically enriched in the microglia cluster (P_{NOM}=3.148E-145; P_{ADJ}=9.4634E-141). We also compared our results with similar recent human prefrontal cortex snRNAseq datasets (Habib et al., 2017; Lake et al., 2016; Lake et al., 2018). In BA9 (n=3) (Habib et al., 2017), expression was also highest in microglia and excitatory neurons (Figure 4a). In the adjacent BA6/BA10 areas (n=6)(2018), highest levels were observed in excitatory and inhibitory neurons (Figure 4a). In the two additional datasets, *FKBP5* expression was not significantly enriched in any of the cell-types, in line with the fact that *FKBP5* is expressed in different cell-types without necessarily defined cell-type identity. High expression in excitatory neurons was a consistent finding across the three datasets.

We subsequently performed triple-label fluorescent immunohistochemistry in Series 3 to examine FKBP51 cellular distribution at the protein level. FKBP51 was colocalised with neuronal marker NeuN, with strong staining present in the cytoplasm and moderate staining in the nucleus (Figure 4b). However, contrary to gex, we did not observe co-localisation of FKBP51 with microglia (TMEM119) nor astrocytes (GFAP) using multiple validated FKBP51 antibodies (Supplemental Table 5, Figure S1a). There was no visible FKBP51 staining in the white matter, suggesting FKBP51 protein is lowly expressed in oligodendrocytes. These data suggest that at the protein level, FKBP51 expression in BA9 is enriched in neuronal subtypes while RNA expression may also be present at detectable levels in microglia and astrocytes.

In the snRNAseq data from Series 4, we next assessed case-control differences of *FKBP5* gex within each of the 26 major cell-type clusters. We observed a marked increase in *FKBP5* gex in the excitatory neuron group in cases with depression compared to controls (+24.8%) after covarying for a strong effect of age (t=-2.327, P_{NOM}=0.0267, effect of corrected age covariate: t=7.130, P=5.18e-08) (Figure 4c), although this did not survive correction for multiple cell-type comparisons (P_{FDR}=0.2548; Supplemental Table 12). There were no significant depression/control differences between *FKBP5* gex in any other cell-type groups, including the microglia cluster (P_{NOM}>0.187). To further narrow down which excitatory neurons contribute to increased *FKBP5* gex, we performed a subsequent analysis in 7 excitatory neuron sub-clusters. Our results showed 25% higher *FKBP5* gex in case vs controls, exclusively in the Ex 10 cluster representing excitatory neurons specifically from superficial cortical layers 2-4 (t=-2.190, P_{NOM}=0.0364), suggesting the increase in *FKBP5* gex in excitatory neurons is specific to neurons of the superficial cortical layers (Supplemental Table 12).

Age influences *FKBP5* and FKBP51 expression specifically in superficial-cortex excitatory neurons

We next examined aging effects of *FKBP5* gex cell-type specifically, by correlating *FKBP5* gex and age in all major cell-type clusters in Series 4 (Figure 5a, Supplemental Table 13). We observed a strong, positive association of *FKBP5* gex with aging in the excitatory neuron group (R=0.664, P_{FDR}=1.31E-04), with weaker effects surviving multiple correction observed in astrocyte and oligodendrocyte cell clusters (R=0.401, P_{FDR}=0.048 for both clusters) but no significant correlation with age in microglia. Further assessment of the excitatory neuron subclusters revealed that the aging effect was specific to, and strongest in, the superficial layer 2-4 excitatory neurons (R=0.700, P_{FDR}=2.88E-05).

Leveraging single-molecule fluorescent *in situ* hybridization with RNAscope assays, we quantified the aging-related changes of *FKBP5* in spatial context with increased accuracy (Series 3), assessing the association of *FKBP5* gex with age in the superficial (Layer II-III) versus the deep layers (V-VI) of the BA9 cortex (Figure 5b). Our results showed a positive correlation of *FKBP5* gex and age specific to the superficial layers of the cortex (R=0.427, P_{NOM}=0.038), but not the deep layers (Figure 5c). Similar to our immunohistochemistry assays, we did not observe *FKBP5* gex in the white matter. The superficial layers of the BA9 cortex consist of small, medium, large and super large pyramidal cells, whereas the deeper layers consist of fewer and smaller pyramidal cells and high density of glia (Figure 5b). These results thus consistently suggest that the disease and aging-related *FKBP5*/FKBP51 increases we observed in the human BA9 cortex are pronounced in excitatory neuron subtypes, and especially those in the superficial cortical layers of BA9.

***FKBP5* co-expression and pathway enrichment differs in younger vs older subjects**

We next aimed to provide broader understanding of the cellular processes altered in association with increased *FKBP5* gex over the life-course. In Series 1, we separated all subjects into three age quantiles and performed gene co-expression analyses in association with *FKBP5* to compare gene sets between subjects in the 1st vs 3rd age quantile (1st quantile: mean 32.17 years, 3rd quantile: mean 54.67 years; n=72 in each quantile). We confirmed that *FKBP5* gex was +47% higher in 3rd vs 1st age quantile (mean *FKBP5* gex 1st quantile = 1.079, mean *FKBP5* gex 3rd quantile = 2.042). In the 1st quantile, 1456 genes were co-expressed with *FKBP5*, while 480 genes were co-expressed with *FKBP5* in the 3rd quantile at FDR 5% (Figure 6a). 221 genes were co-expressed in both age groups, but the majority of genes were uniquely co-expressed in each age quantile. We used WebGestalt with these shared or uniquely expressed genes as input to perform functional gene ontology (GO) enrichment analyses (GO:Biological Process) of co-expression partners in each quantile to relate the genes co-

expressed with *FKBP5* to biological functions (FDR 5% and >15 genes per pathway; Figure 6b). Overall, genes and the corresponding pathways in the 1st quantile displayed independent relationships compared to genes uniquely co-expressed in the 3rd quantile, and the intersecting genes between the two quantiles appeared to be driven by age.

Of the shared genes co-expressed with *FKBP5* in both age quantiles, significantly enriched processes included positive regulation of cytokine production defence, defence response to other organisms, regulation of inflammatory response, positive regulation of defence response, positive regulation of secretion, and regulation of peptide secretion. The transcripts within these terms were positively correlated to *FKBP5* gex (75% to 100% of transcripts within pathway, Figure 6c). Of the transcripts uniquely co-expressed between the 1st and 3rd quantiles, we also saw that significantly enriched processes mainly included transcripts that had a positive correlation to *FKBP5* gex (1st: 76-100%, 3rd: 75-100% of transcripts within the pathway, Figure 6c), but the terms were distinct between the two age groups. In the 1st quantile, we saw enrichment of *FKBP5* co-expression with genes involved in terms relating to synaptic plasticity, including in neuron projection organisation and dendrite development, as well as regulation of vesicles and synaptic functions. The co-expression patterns in the third-age quantile were enriched in GO terms mainly related to various aspects of immune signalling and apoptosis. The vast majority of transcripts included in these processes were up-regulated (log2 FC > 0) in cases compared to controls (Figure 6d). These data indicate that there are distinct functional consequences of increased *FKBP5* gex depending on age and that transcripts co-expressed with *FKBP5* show differences in expression between cases and controls, most pronounced for co-expression in the older age group.

DISCUSSION

This study describes the largest and most comprehensive study to date aimed at elucidating the factors that associate with *FKBP5* mRNA and FKBP51 protein expression in the human BA9 dorsolateral prefrontal cortex, and how *FKBP5* and FKBP51 is affected in severe psychiatric disorders. Our results demonstrate that case-status, age and genotype intersect to modulate the levels of *FKBP5* and FKBP51 expression in this brain area, and that this could be mediated by convergent epigenetic effects on functional upstream enhancers. *FKBP5* displays a distinct cell-type specific expression pattern, and effects of case- and age- status appear to be particularly pronounced in excitatory neurons of the superficial layers of BA9. Importantly, increased *FKBP5* expression associates with distinct pathways according to age, specifically synaptic plasticity pathways in early adulthood, and brain aging and neuroinflammatory pathways in subjects over 50 years. In addition, genes positively co-expressed in older individuals were also upregulated in cases compared to controls, suggesting that FKBP51 antagonists in older patients may have utility to attenuate brain aging and neuroinflammation. Together, these results indicate that the heightened *FKBP5* cortical expression observed in psychiatric patients accumulates over the life course to eventually cross a pathological threshold with widespread and broad physiological consequences that likely contributes to the pathobiology of psychiatric disorders, at least in a subset of patients. Our data indicate that the aging pattern of expression is exacerbated particularly in rs1360780 risk-allele carriers with schizophrenia and major depression at older ages, providing the first evidence that this specific subgroup of psychiatric patients (risk-allele carriers over 50 years of age) may benefit most from FKBP51-antagonist treatment.

Case-status and age both associate with lower DNAm within a proximal enhancer that contains a series of GREs (Wiechmann et al., 2019) and for which lower DNAm correlates with higher *FKBP5* expression (see Figure 3c and Figure 3d). It has been shown that activation of the stress-hormone receptor via the synthetic agonist dexamethasone leads to reduced DNAm at this same enhancer in peripheral blood cells as well as a human hippocampal neuronal progenitor cell line (Provençal et al., 2020; Wiechmann et al., 2019). Convergent associations of GR agonist treatment and exposure to childhood adversity on DNAm at the *FKBP5* locus have been reported in intronic GREs (Klengel and Binder, 2013). While it is plausible that stress and adversity, via activation of the stress hormone system, could also impact DNAm of this enhancer, this has not yet been explored in the context of childhood adversity. There could thus be convergence of environmental exposures and risk genotype on brain-expressed *FKBP5* via epigenetic effects on this enhancer, in line with more than 31 independent studies performed in over 31,000 individuals, consistently indicating that carriers of the *FKBP5* risk haplotype who are exposed to childhood adversity are at increased trans-diagnostic risk for developing severe psychopathology (Matosin et al., 2018). It is important to note that there may be effects of medication, especially antidepressants, in cases, given that reductions in blood *FKBP5*

mRNA and protein expression during antidepressant treatment has been reported(Ising et al., 2019). Our finding is thus likely to be conservative, with unmedicated patients likely to show even more exacerbated effects.

Until now, *FKBP5*/FKBP51 cell-type distribution and expression patterns in the human brain have been largely unknown. We show that *FKBP5* is most consistently expressed in excitatory neurons at the mRNA and protein levels, and that case-status (specifically depression) and age effects are most pronounced in excitatory pyramidal cells in the superficial cortical layers of BA9, although larger single-nucleus datasets with more power could reveal additional effects. While we also observed high expression in microglia in our BA9 single-nucleus RNA sequencing dataset, microglia-specific *FKBP5* expression was not different in cases vs controls and was not associated with age. FKBP51 protein expression was also absent in microglia using two validated FKBP51 antibodies. Of note, in total more microglia (and nuclei in total) were captured from cases compared to controls (480 vs 372 respectively (Nagy et al., 2020)), which could contribute to the increased *FKBP5* gex observed overall given microglia appear to be high expressors of *FKBP5* mRNA. However, it is also possible that microglia-associated *FKBP5* expression may be reflective of increased microglia numbers which is suggested to occur in psychiatric disorders (Kaul et al., 2021), although a factor not explored in this study.

The alteration of *FKBP5* expression in excitatory neurons is of functional importance, given that knock-out of *Fkbp5* in mice has been shown to decrease long-term potentiation and increase presynaptic GABA release (Qiu et al., 2019). Transgenic mice overexpressing the human FKBP51 display impaired long-term depression as well as spatial reversal learning and memory. This may be mediated via effects of *FKBP5* on chaperone-mediated recycling of α-amino-3-hydroxy-5-methyl-4-isoxazolepropionic acid (AMPA)-receptors, with high *FKBP5* accelerating the rate of AMPA recycling and thus altering AMPA receptor trafficking (Blair et al., 2019). Furthermore, increased *FKBP5* expression has been correlated with reduced mushroom and overall spine density (Young et al., 2015). This suggests that increased glucocorticoid-related *FKBP5* expression may in part also mediate the reported effects of glucocorticoids in the prefrontal cortex of rodents, the functional homologue to the dorsolateral prefrontal cortex of humans, where glucocorticoids have vast effects on working memory, memory consolidation and cognitive flexibility (Barsegyan et al., 2010; Myers et al., 2014). Impaired cognition is a transdiagnostic symptom frequent in all the investigated psychiatric disorders in this study, and often associated with a worse prognosis (McTeague et al., 2016). Targeting symptoms in the cognitive domain are thus of particular clinical interest.

We showed that the functional consequences of increased *FKBP5* varies across the lifespan, with heightened cortical-*FKBP5* in young adults associated with altered synaptic transmission, whereas in

older individuals, heightened cortical-*FKBP5* was related to increased neuroinflammation and neurodegeneration. Possible impact of *FKBP5* on synaptic transmission in younger individuals is consistent with the neuronal expression pattern reported above as well as direct protein/protein interaction partners and downstream targets of FKBP51 that have been shown to impact neuronal function. These include brain-derived neurotrophic factor (BDNF)(Anderzhanova et al., 2020), glycogen synthase kinase 3ß (GSK3ß)(Gassen et al., 2016a), calcineurin (Baughman et al., 1995; Matthias Weiwad et al., 2006), synapsin (Schmidt et al., 2015), protein kinase B/Akt (Fabian et al., 2013) and AMPA receptors (Blair et al., 2019). In older individuals, we observed co-expression of *FKBP5* with gene transcripts in pathways related to neuroinflammation and neurodegeneration. These effects again are likely mediated by direct or downstream targets of FKBP51. We have previously reported that increased FKBP51 contributes to a proinflammatory profile with increased age via activation of the alternative nuclear-factor$_K$B (NF_KB) pathway (Zannas et al., 2019). In addition, increased feedforward signalling related to the reported interactions of *FKBP5* with tau, the mammalian target of rapamycin (mTOR) and protein kinase B (Akt)(Blair et al., 2013; Gassen et al., 2015; Gassen et al., 2016b), may also contribute to these effects. Finally, FKBP51 has also been shown to play an important role in priming autophagy (Gassen et al., 2014; Rein, 2016), in line with the co-expression of *FKBP5* with neurodegenerative pathways. Given that most of the co-expressed transcripts enriched in inflammatory and brain aging related pathways showed a positive correlation with *FKBP5* and were predominately upregulated in cases, older patients with heightened *FKBP5* expression may specifically benefit from treatments reducing FKBP51 activity.

Integrating multiple postmortem brain cohorts and analyses approaches, this study provides insight into brain *FKBP5*/FKBP51 expression in the human brain and its utility as a drug target and biomarker for a specific subtype of patients most likely benefiting from FKBP51-targeting treatment. Our data suggest that patients with severe psychiatric disorders, particularly those with schizophrenia and major depression over the age of 50 who carry the *FKBP5* risk haplotype, could represent a patient subgroup that are likely to benefit most from FKBP51 antagonists. These findings answer an international call for molecular psychiatry approaches that reclassify psychiatric diagnoses based on biology, rather than symptomatology (Visscher et al., 2017). Future brain studies that include environmental influences, particularly early life adversity, as well as the connection between *FKBP5* expression in the periphery and brain, are now needed.

ACKNOWLEDGEMENTS

We thank the families from the USA, Canada, Germany and Australia who donated brain tissues to this research. We specifically thank the Lieber and Maltz families for their contributions towards the Lieber Institute brain collection. The Douglas-Bell Canada Brain Bank is funded by the Réseau Québécois sur le suicide, le troubles de l'humeur et les troubles associés (FRQS) as well as by Healthy Brains for Healthy Lives (CFREF) and Brain Canada grants to Dr Turecki and Dr Mechawar. The Victorian Brain Bank tissue collection was supported by the National Health and Medical Research Council (NHMRC; Australia; grant number 566967) and the Cooperative Research Centre (CRC) for Mental Health and the Operational Infrastructure Support from the Victorian State Government. We would additionally like to thank Geoff Pavey for his efforts in curating the Australian Victorian Brain Bank and Madhara Udawela for supervising preparation of brain tissues in series 2. Dr Matosin was supported by an Al and Val Rosenstrauss Fellowship from the Rebecca L Cooper Medical Research Foundation, an NHMRC Early Career Fellowship (APP1105445), Alexander von Humboldt Foundation Research Fellowship, and International Brain Research Organisation (IBRO) Research Fellowship. Dr Matosin was also supported by grants from the Brain Behaviour Research Foundation (NARSAD Young Investigator Grant, #26486) and the Rebecca L. Cooper Medical Research Foundation (#PG2020645). Dr Arloth was supported by the Brain Behaviour Research Foundation (NARSAD Young Investigator Grant, #28063). Dr Mechawar's research is supported by grants from CIHR, HBHL and ERA-NET NEURON. Dr Gassen was supported by a grant from the Brain Behaviour Research Foundation (NARSAD Young Investigator Grant honoured by the P&S Fund #25348).

AUTHOR CONTRIBUTIONS

N.Ma. and E.B.B. conceived, designed and managed the work, performed all intitial analyses and drafted the manuscript. J.A., D.C., M.M., T..H, R.T. and A.E.J. were all involved in conceptualising and assisting with the statistical analyses. J.A., D.C., T.H. and C.C. were also involved in substantively drafting and revising the work. S.M., D.K., N.C.G., K.H. performed immunoblot and histological analyses, and assisted with interpretation of this data. N.S.M., K.W., G.R., C.N. were involved preparation of omics data for statistical analyses. E.S., T.A., P.F., J.E.K., D.R.W., N.Me., A.S,. B.D., G.T., and T.M.H. were all involved in collection, dissection and curation of the brain samples used in this study, as well as managing the experiments and sharing the resulting datasets. All authors were involved in the acquisition, analysis and interpretation of the data, and approved the final version of the manuscript.

DECLARATION OF INTERESTS

Dr Binder is co-inventor on the following patent applications: FKBP5: a novel target for antidepressant therapy. European Patent# EP 1687443 B1; Polymorphisms in ABCB1 associated with a lack of clinical response to medicaments. United States Patent # 8030033; Means and methods for diagnosing predisposition for treatment emergent suicidal ideation (TESI). European application number: 08016477.5 International application number: PCT/EP2009/061575. Dr Falkai has been an honorary speaker for AstraZeneca, Bristol Myers Squibb, Eli Lilly, Essex, GE Healthcare, GlaxoSmithKline, Janssen Cilag, Lundbeck, Otsuka, Pfizer, Servier, and Takeda. During the past 5 years, but not presently, P. Falkai has been a member of the advisory boards of Janssen-Cilag, AstraZeneca, Eli Lilly, and Lundbeck. Dr Schmitt has been an honorary speaker for TAD Pharma and Roche and has been a member of advisory boards for Roche. The remaining authors declare no competing interests or conflicts of interest.

FIGURE LEGENDS

Figure 1. ***Hypothesised model of* FKBP5/*FKBP51 expression and DNAm aging trajectories over the life course, and how these are influenced by genes and environment to contribute to the development of psychopathology later in life.*** Extensive data from human genetic, animal and epidemiological studies indicates that carriers of the *FKBP5* high induction haplotype (**a**) have increased *FKBP5*/FKBP51 expression (**b**) over the life-course. This is likely to be related to changes in DNAm at functional genomic sites of the *FKBP5* gene (**c**), which occurs in patients exposed to early life adversity (**d**). The combined genetic and epigenetic disinhibition of *FKBP5* is hypothesised to cause heightened expression patterns over the life course (teal compared to red curves). This heightened aging trajectory is hypothesised to enter an abnormal range (**e**) to contribute to a dysregulated stress response and increased risk to psychopathology later in life. It is proposed that treatment with FKBP51 antagonists, especially during critical life-stages such as that indicated (**f**), is a promising therapeutic approach to correcting heightened FKBP5 expression levels to prevent the development of psychopathology, or treat symptoms, in a patient subset (**g**): specifically carriers of the high induction *FKBP5* haplotype who are exposed to early life adversity.

Figure 2. ***Case-control differences in* FKBP5 *gene expression, and FKBP51 protein, and effects of age.*** **(a)** *FKBP5* gene expression was increased in all cases (grouped) compared to controls in Series 1 (left) and Series 2 (middle). The same pattern of expression was seen at the protein level in Series 2 (right). Significance bars compare all cases compared to controls. **(b)** *FKBP5* gene expression and FKBP51 protein were strongly and positively correlated in all subjects in Series 2. **(c)** Lifetime trajectory of *FKBP5* gene expression in control subjects Series 1, spanning from foetal time points to almost 90 years of age. *FKBP5* gene expression steadily increases over the life course in healthy subjects. **(d)** FKBP51 protein expression increases over adulthood in healthy control subjects from Series 3. **(e)** *FKBP5* gene expression positively correlates with age in cases compared to controls in Series 1, and expression is significantly heightened in schizophrenia and depression compared to controls. **(f)** FKBP51 protein expression in Series 2 is significantly heightened in cases compared to controls over aging. Comparison of individual diagnostic groups (schizophrenia, major depression and bipolar disorder vs controls) were not included due to limited power. *Abbreviations:* BPD, bipolar disorder; CTL, control; gex, gene expression; MDD, major depressive disorder; SCZ, schizophrenia; Series refer to the cohorts used for each analyses, as detailed in Table 1. Asterix indicate significance levels: *P<0.05, **P<0.01, ***P<0.001.

Figure 3. ***Effects of genotype and age on* FKBP5 *expression and DNA methylation.***

(a) Effects of the *FKBP5* risk haplotype (tagged by the rs1360780 T allele) on gene expression. Case T carriers displayed significantly higher gene expression levels compared to control CC homozygotes and control T carriers, but not case CC homozygotes. **(b)** The aging trajectory of *FKBP5* gene expression was significantly different between genotype groups, with increased expression in case T allele carriers compared to control CC homozygotes (scatterplot). This was specifically due to increased gene expression in case T allele carriers compared to control CC homozygotes at ages 50-75 years (boxplot). **(c)** Relationships between *FKBP5* DNA methylation and gene expression in Series 1. *FKBP5* DNA methylation in the downstream conserved region and the proximal enhancer (total) were negatively associated with gene expression. **(d)** Corrplot summarising correlations of age, *FKBP5* total gene expression and DNA methylation (CpG groupings as per Supplementary Table 8) in Series 1 across all subjects aged 14-75 years old. *Abbreviations:* BPD, bipolar disorder; CTL, control; Ca_CC, case CC genotype carriers; Ca_T, case T allele carriers; Co_CC, control CC genotype carriers; Ca_T, case T allele carriers; distal TAD, distal topologically associated domain; DNAm, DNA methylation; Downstr Cons, downstream conserved region; gex, gene expression; MDD, major depressive disorder; GRE, glucocorticoid response element; SCZ, schizophrenia; TSS, transcription start site; Prox Enh Tot, total DNAm across the total proximal enhancer region; Prox TAD, proximal topologically associated domain. Series refer to the cohorts used for each analyses, as detailed in Table 1. Asterix indicate significance levels: *P<0.05, **P<0.01, ***P<0.001.

Figure 4. ***Cell-type specificity and distribution of* FKBP5*/FKBP51 expression in BA9***. **(a)** Dot plots indicating average expression of *FKBP5* in cell-type clusters derived from single-cell RNA-sequencing data across three cohorts: (i) Series 4, (ii) Habib et al., (iii) Lake et al. *FKBP5* expression was visually enriched on microglia in cohorts (i) and (ii), and astrocytes in cohorts (i) and (iii). *FKBP5* mRNA was consistently expressed on excitatory neuron subtypes across all three cohorts. **(b)** Triple-label immunohistochemistry of FKBP51 protein in Series 3. FKBP51 was colocalised with NeuN (neuronal marker), but not GFAP (astrocytes) or TMEM119 (microglia). **(c)** Cell-type specific differences in *FKBP5* gene expression in cases vs controls in Series 4. *FKBP5* expression was significantly higher in cases (all cases of depression) vs controls in the excitatory neuron cluster, specifically due to increased levels of expression in excitatory neurons from the superficial cortical layer (layer 2-4). Asterix indicate significance levels: *P<0.05. *Abbreviations:* gex, gene expression; Ex, excitatory.

Figure 5. ***Cell-type distribution of* FKBP5*, and cell-type effects of aging on* FKBP5.** **(a)** *FKBP5* was positively correlated with age in oligodendrocytes, astrocytes and excitatory neurons in Series 4. The association in the excitatory neuron cluster was due to a strong correlation specifically in excitatory

neurons from the superficial (layer 2-4), but not deep (layers 5-6), cortical layers. **(b)** Representative images from single-molecule in-situ hybridisation experiments examining *FKBP5* expression (sum of two probes, FKBP5_1 and FKBP5_2) in the superficial (layers 2-4) vs deep cortical layers (layers 5-6) in Series 3. **(c)** Correlation results of *FKBP5* expression with age, quantified from single-molecule in-situ hybridisation experiments in Series 3. *FKBP5* was significantly and positively correlated with age in the superficial, but not the deep cortical layers.

Figure 6. FKBP5 ***co-expression analyses and functional gene ontology enrichment analyses, including effects of age and diagnosis on co-expression.*** **(a)** Venn diagram showing overlap of genes co-expressed with *FKBP5* in young (1st age quartile) vs older (3rd age quartile) subjects from Series 1, with 211 common genes and 1373 uniquely co-expressed genes. **(b)** Heat map illustrating pathways enriched for *FKBP5* co-expression partners across gene sets for the 1st and 3rd quantile, and the genes significantly co-expressed at the intersection between both quantiles. Missing values/pathways, represented in white. **(c)** Enriched pathways of genes uniquely co-expressed with *FKBP5* in the 1st (left) vs 3rd (middle) age quantiles, as well as the genes that intersect between the quantiles (right). Bars indicate a positive (coral) or negative (aqua) correlation with *FKBP5* gene expression. Positive and negative correlations with *FKBP5* were calculated using all samples combined. **(d)** Enriched pathways of genes uniquely co-expressed with *FKBP5* in the 1st (left) vs 3rd (right) age quantiles. Bars indicate a up- (red) or down- (blue) regulation in cases compared to controls. In the 1st age quantile, pathways related to synaptic plasticity functions were predominately downregulated in cases compared to controls, whereas in the 3rd age quantile, pathways related to immune signalling and apoptosis were up-regulated in cases compared to controls. *Abbreviations:* GO:BP, gene ontology biological pathway classification.

METHODS

1. Human postmortem brain samples

FKBP5 gex, DNAm and FKBP51 protein expression were examined in the dorsolateral prefrontal cortex (DLPFC; Brodmann Area 9, BA9) from 895 individuals across four postmortem brain cohorts (Table 1). Series 1 consisted of 668 subjects from the Lieber Institute for Brain Development Repository, with the study protocol approved by the NIMH/NIH Institutional Review Board (protocol 90-M-0142) and the National Institute of Child Health and Human Development Brain and Tissue Bank for Developmental Disorders (http://www.BTBank.org/) under contracts NO1-HD-4-3368 and NO1-HD-4-3383 approved by the Institutional Review Board of the University of Maryland. Subjects included a lifetime cohort of non-psychiatric controls (n=340), spanning in age from the prenatal second trimester to 85 years, and teenagers, adults, and 50+ year old subjects with schizophrenia (n=121), major depressive disorder (n=144) or bipolar disorder (n=63). Series 2 consisted of 169 adult subjects aged 18-87 years with schizophrenia (n=68), major depressive disorder (n=24), bipolar disorder (n=15) and matched controls (n=62). A subset of Series 2, consisting of 76 adult subjects with schizophrenia (n=20), major depression (n=20), bipolar disorder (n=16) or controls (n=20) was used specifically for protein analyses. These tissues were collected at the Victorian Institute of Forensic Medicine and obtained from the Victorian Brain Bank at the Florey Institute for Neuroscience and Mental Health, with approval from the Ethics Committee of the Victorian Institute of Forensic Medicine after gaining written consent from the nearest next of kin. This study was approved by the Human Ethics Committee of Melbourne Health. Series 3 consisted of adult control subjects aged 37-88 (n=24) with no history of psychiatric or neuropathological illness collected at the Neurobiobank at the Ludwig-Maximilians-University, with approval from the Ludwig-Maximilians-University ethics commission (#17-085). Series 4 consisted of 34 adult subjects with major depressive disorder (n=17) and matched controls (n=17) obtained from the Douglas–Bell Canada Brain Bank, approved by the Douglas Hospital Research Ethics Board with written informed consent from next of kin for each individual. Extensive details regarding cohort collection and tissue dissection methods for each series are included in the Supplemental Materials and Supplemental Tables 1-4.

Table 1. Summary of cohorts, methods, and analyses conducted.

Series	Diagnosis (n)	n	Age range (years)	Sex (M/F)	Method	Analyses
Series 1 *Lieber Institute for Brain Development, USA*	*All Controls:* lifetime sample, prenatal to adult	340	14weeks-85	228/112	Bulk RNA sequencing	Lifetime *FKBP5* gex (all controls)
	Case-control: Controls: subset of all control subjects >14 years	179	14-85	137/42		Case-control differences in *FKBP5* gex
	Schizophrenia	121	17-96	80/41		Case-control differences in *FKBP5* gex aging trajectories
	Major Depression	144	14-75	87/57		
	Bipolar Disorder	63	21-76	35/28		
					DNA methylation array	Case-control differences in *FKBP5* DNAm
						Case-control differences in *FKBP5* DNAm aging trajectories
					SNP genotyping	Effects of rs1360780 SNP on *FKBP5* gex and DNAm
						Effects of rs1360780 SNP on *FKBP5* gex and DNAm aging trajectories
Series 2 *Victorian Brain Bank at the Florey Institute for Neuroscience and Mental Health, AUS*	Controls	62	22-80	49/13	Exon array	Case-control differences in *FKBP5* gex
	Schizophrenia	68	18-82	54/14		
	Major Depression	24	19-87	12/12		Case-control differences in *FKBP5* gex aging trajectories
	Bipolar Disorder	15	31-79	7/8		
	Controls	20	32-80	11/9	Immunoblot	Case-control differences in FKBP51 protein
	Schizophrenia	20	30-82	11/9		
	Major Depression	20	27-87	11/9		Case-control differences in FKBP51 protein aging trajectories
	Bipolar Disorder	16	31-79	8/8		
						Correlation of *FKBP5* gex (exon array) and FKBP51 protein levels in the same subjects
Series 3 *Neurobiobank at the Ludwig-Maximilians-University, GER*	Controls	24	37-82	13/11	Quantitative PCR	*FKBP5* gex aging trajectory in controls
					Immunoblot	FKBP51 protein aging trajectories in controls
						Correlation of *FKBP5* gex (qPCR) and FKBP51 protein levels in the same subjects
					Single-molecular in-situ hybridisation (RNAscope)	Cortical layer specificity of *FKBP5* long- and short- variants
						Layer-specific aging trajectories of *FKBP5* long- and short- variants
					Immunohistochemistry	*FKBP5* cellular and subcellular distribution across neurons, microglia and astrocytes in the grey matter
Series 4 *Douglas–Bell Canada Brain Bank, CA*	Controls	17	18-87	34/0	Single-nucleus RNA sequencing	*FKBP5* specificity to distinct cell-type clusters
	Major Depression	17	19-82			Case-control differences in *FKBP5* gex across cell-type clusters

Series 1

2. RNA sequencing

RNA sequencing methods have been previously described (Tao et al., 2017). Briefly, total RNA from postmortem brain Series 1 was extracted using RNeasy Lipid Tissue Mini Kits (Qiagen, Germantown, MD, USA). RNA was then purified with RNeasy Mini Spin columns including on-column DNase digestion (Qiagen). Total RNA yield was determined with Qubit (ThermoFisher Scientific, Waltham, MA, USA) and RNA quality and RNA integrity assessed with the Agilent Bianalyzer 2100 (Agilent Technologies, Santa Clara CA USA). Poly-A containing RNA was purified from 1μg total RNA and

mRNA molecules fragmented using divalent cations and heating. cDNA conversion was achieved with reverse transcriptase and random hexamers, and second-strand cDNA was synthesized with DNA polymerase 1 and RNase H. T4 DNA polymerase, T4 polynucleotide kinase (PNK0), and Klenow DNA polymerase were applied for end-repair. The addition of an 'A' base was achieved using Klenow Exo (3' to 5' exon minus) and ligation of Illumina P adapters to allow for pooling <8 samples in one flow cell. Purification and enrichment were then achieved by PCR to create the final cDNA library. High-throughput sequencing was performed on the HiSeq 2000 (Illumina, San Diego, CA, USA), with the Illumina Real Time Analysis module used for image analysis and base-calling and the BCL Converter (CASAVA v1.8.2) to generate FASTQ files with sequencing pair-end 100 bp reads.

Splice-read mapper TopHat (v2.0.4) was used to align reads to the human genome reference (UCSC hg19), with known transcripts provided by Ensembl Build GRCh37.67. Mapped reads covering the genomic region of *FKBP5* (chr6:35541362-35696397, GRCh37/hg19) were acquired. Reads covering each exon or unique exon-exon junction level were called using featureCounts (V1.5.0) (Liao et al., 2013). Individual raw exon and junction reads were divided by the mapped total reads per subject. To remove residual confounding by RNA degradation, we used the quality surrogate variable analysis (qSVA) framework previously described (Jaffe et al., 2017).

3. DNA methylation microarray

DNAm methods have been previously described (Jaffe et al., 2016). Briefly, genomic DNA from postmortem brain Series 1 was extracted from 100mg of pulverized DLPFC tissue using phenol-chloroform. 600ng of genomic DNA was bisulfite converted with the EZ-DNA methylation kit (Zymo Research, Irvine, CA, US). DNAm was assessed using the Illumina HumanMethylation450 BeadChip kit which covers >485,000 CpG dinucleotides (cg) covering 99% RefSeq gene promoters, including the *FKBP5* gene promotor. Arrays were run according to the manufacturer's protocols, with a percentage of the samples run in duplicate across multiple processing plates for assessing technical variability due to DNA extraction and bisulfite conversion. DNAm data was processed and normalized using Bioconductor's Minfi package in R (Aryee et al., 2014). Batch effects were corrected as previously described, with batch-derived principle components used as covariates(Jaffe et al., 2016). Cell-type composition was also estimated for relative proportions of cell-types (neuronal and non-neuronal) using epigenome-wide DNA methylation data as previously described (Jaffe et al., 2016).

4. SNP genotyping

Genomic DNA from postmortem brain Series 1 was extracted from 100mg of pulverized cerebellum tissue with the phenol-chloroform method. SNP genotyping was performed with the HumaHap650Y_V3 or Human 1M-Duo_V3 BeadChips (Illumina) according to manufacturer's instruction as previously described (Tao et al., 2017). The rs1360780 *FKBP5* single nucleotide

polymorphism (SNP) was extracted from the dataset. This SNP has been shown to affect *FKBP5* chromatin shape and transcription (Klengel and Binder, 2013).

5. Statistical methods for case-control and aging analyses in Series 1

Analyses were performed in R v3.3.1 (https://www.r-project.org). Potential confounding factors (demographic and clinical variables) were screened using correlational analyses, and subsequently used as covariates or taken into account into residuals in the subsequent models. For gex and DNAm analyses, confounding factors included age (except for age-specific analyses), sex, race, and postmortem interval (PMI). For gex, qSVA principle component variables were also included as covariates to account for RNA degradation(Jaffe et al., 2017). For DNAm, batch correction variables (for independent sample processing) and neuronal/non-neuronal cell-type estimations were additionally included. Case-control differences in gex and DNAm according to diagnosis and/or genotype were assessed using linear regressions including screened covariates. For gex analyses, unique exon-exon junction reads specific to all transcripts were assessed (35565181-35586872, hg38).

Gex and DNAm aging trajectories over the lifetime were analysed using logistic regression and Local Polynomial Regression (LOESS) fitted curves with the ggplot package in R. Gex and DNAm age trajectories were compared between diagnostic or genotype groups using the R package *sm* and the test for equality of non-parametric regression curves available in the sm.ancova command (Bowman and Azzalini, 1997; Young and Bowman, 1995). As *sm.ancova* does not accept covariates, we calculated the residuals of a linear model with the screened covariates with these residuals then used as response values in *sm.ancova*. Logistic regressions and partial correlations accounting for screened covariates were used to determine correlational relationships between gex, DNAm, genotypes and age, with linear or non-parametric modelling dependent on which model could best explain data variability. Interaction analyses of genotype and cases-status were specifically analysed using the approach previously described (Kraft and Aschard, 2015). For age analyses, post-hoc analyses were performed to confirm differences in age-trajectories at different ages with *lm* analyses, assessing case-control or genotype differences within individual age groups (teens, adults, 50+ age groups). Subjects 14-100 years were included in case-control analyses, given the youngest case (depression) was 14 years old. Ages were limited to 14-75 years when assessing genotype to ensure sufficient power, specifically with five subjects per diagnostic group and age range (teen, adult, 50+ age groups). Multiple-testing correction was applied using a FDR cut-off value of 0.05 (Benjamini and Hochberg, 1995), unless otherwise noted.

6. Gene co-expression and pathway analyses in Series 1

To find genes co-regulated with *FKBP5*, we regressed the gene expression levels of *FKBP5* against the expression of all other genes correcting for age, sex, race, PMI and PC1-PC7 (qSVAs). Multiple

comparisons correction was performed using the Benjamini–Hochberg procedure with a corrected false discovery rate (FDR) cut-off of 0.05. Using the set of FDR-corrected genes, gene ontology enrichment analysis was performed using the WEB-based GEne SeT AnaLysis Toolkit (http://www.webgestalt.org/) with "Biological Process noRedundant" set as the database and the set of 24,793 genes as background. GO terms with at least 15 genes and FDR < 0.05 were considered as significant.

Series 2

7. Exon arrays

This method has been previously described (Scarr et al., 2018). Briefly, total RNA was isolated using TRIzol reagent (Life Technologies, Scoresby, VIC, Australia) and RNeasy mini kits (Qiagen, #74104, Chadstone Centre, VIC, Australia). RNA quality and quantity were assessed and samples with RINS of 7 or greater were deemed suitable for further analyses with the Affymetrix Human Exon 1.0 ST Array according to the manufacturer's instructions (Affymetrix, Santa Clara, CA, USA). After hybridisation, chips were scanned and the fluorescent signals converted into a DAT file for quality control, and CEL and CHP files were generated. Exon array data was used as a replication for the RNAseq gex analyses in Series 1 and followed the same statistical methods. For *FKBP5* gex measures, we analysed signal from *FKBP5* exon 5 (ENSE00000747342.1) which sits adjacent to the *FKBP5* exon-exon junction used to assess total *FKBP5* gex in Series 1.

8. Immunoblot (Series 2 and 3)

Relative protein densities of FKBP51 were determined by immunoblot in postmortem brain Series 2 and Series 3 as previously described (Matosin et al., 2015). 10mg of grey matter from each block was homogenised and protein concentration determined using BCA assays. For each sample, 12µg protein was denatured at 95°C in sample loading buffer consisting of Laemmli buffer and β-mercaptoethanol for 5mins. Duplicate samples were then loaded in a randomized order across four bis-tris polyacrymalide gels (4–20% Mini-PROTEAN TGX Precast 15-well Protein Gels, #4561096, BioRad, Hercules, CA, USA), at a loading concentration of 20µg of total protein per lane. Protein ladder (Precision Plus Protein Dual Colour Standard, BioRad) and a pooled sample (to account for gel-to-gel variability) were loaded onto each gel. Proteins were separated via electrophoresis with tris-glycine SDS buffer (BioRad) at 200V for 30mins. Separated proteins were transferred onto PVDF membrane (BioRad) at 100V at 4°C for 35min using Tris-glycine buffer (BioRad) containing 20% methanol. Transfer efficiency was confirmed using Ponceau S stain (Sigma-Aldrich), followed by washes in tris-buffered saline with Tween 20 (TBST). Membranes were blocked with 5% skim milk in TBST for 1hr at room temperature. Membranes were then incubated overnight at 4°C with selected primary antibody (Supplemental Table 5) diluted with TBST containing 1% skim milk. Primary antibody specificities were validated in FKBP51 knock out (KO) cells, generated from the SH-SY5Y human neuroblastoma

cell line using CRISPR-Cas9 (Figure S1). Following primary incubation, blots were washed and incubated for 1hr at room temperature with horse-radish peroxidase-conjugated secondary antibody (anti-rabbit: 1:3000), washed and visualised using enhanced chemiluminscent detection. Band density was detected by the BioRad ChemiDoc XRS+ (Series 2) or the Amersham 6000 Gel Imager (GE Healthcare, Series 3) and quantified with Image Lab Software (BioRad). Membranes were re-probed a loading control (Series 2: anti-β-actin polyclonal antibody Santa Cruz Biotechnology, Dallas, TX USA #sc-1616, 1:3000; Series 3: glyceraldehyde 3-phosphate dehydrogenase Abcam #ab9485, 1:2500). Densitometry values for each sample was normalised to the respective loading control, then to the respective pooled sample to account for gel-to-gel variability. Duplicates were averaged for each sample, and the mean of the two primary antibodies taken as the final values. Normalised protein levels were assessed for normal distribution and correlated with age and qPCR gex values using partial spearman correlations in R, as well as the *nlcor* package in R, a nonlinear correlation estimator (Ranjan and Najari Sisi, 2019).

Series 3

9. Quantitative Real-Time PCR

mRNA levels of *FKBP5* transcripts in Series 3 were measured using qRT-PCR. 40mg of grey matter was dissected from each tissue block. RNA was extracted and RIN quantified as for RNA sequencing in Series 1. cDNA was synthesised from 500ng of RNA using the Maxima H Minus Reverse Transcriptase system (ThermoFisher Scientific). PCR conditions were set to 94°C for 5min, 40 cycles of 94°C for 30 s, 60°C for 30 s, 72°C for 30 s, and 72°C for 7min after the last cycle. Primer pairs were designed to amplify the unique junctions for total *FKBP5* gex (Supplemental Table 6), using customized TaqMan Gene Expression Assays (Applied Biosystems, Foster City, CA, USA) and the Lightcycler 480 (Roche, Basel, Switzerland). Gex levels of *FKBP5* was normalized to geometric means of the constitutively expressed genes β-actin (ACTB) and glyceraldehyde-3-phosphate dehydrogenase (GAPDH). Samples were measured in quadruplicate and averaged. Normalised mRNA levels were then checked for normal distribution and correlated with age using spearman correlations in R.

10. Single-molecule fluorescent in situ hybridisation

To quantify the gex and examine cortical localisation of *FKBP5* alternative transcripts, single-molecule fluorescent in situ hybridisation was performed in Series 3 using the RNAscope Fluorescent V2 kit (Advanced Cell Diagnostics, Newark, CA, USA). The tissue preparation was conducted according to the manufacturer's instructions for the RNAscope® Part 1, Fresh Frozen Tissues protocol, with minor modifications for increased signal-to-noise ratio. Briefly, the 24 tissue blocks from Series 2 were cryosectioned at 16µm and mounted onto Superfrost Plus Gold slides. In situ hybridisation was performed in duplicate, using adjacent sections for each subject. Sections were post-

fixed with 4% PFA for 1 hr at 4°C and washed in wash buffer. Slices were permeabilised with hydrogen peroxide for 10min and digested with protease IV for 30min. The slices underwent the hybridisation procedures using the RNAscope® Multiplex Fluorescent Version 2 User Manual Part 2 (ACD), with wash steps increased to 3x between each hybridisation step and signal amplification to reduce background signal. We used two hybridisation probes customised to target either (1) *FKBP5* long transcripts (V1-3) in channel 2 at 1000-2041bp, or (2) *FKBP5* short transcript (V4) in channel 3 at 1475-2968bp. Total *FKBP5* gex was then calculated by summing the results of short and long probes together. Positive (POLR2A and PPIB) and negative (DapB) control probes were also included. TSA fluorophores for cyanine 3 and cyanine 5 (Perkin Elmer) were used at a concentration of 1:1000. Slides were counter-stained with DAPI. Lastly, autofluorescence eliminator reagent (Merck Millipore-2160) was applied to reduce fluorescence in the cyanine 3 channel (~570nm), generated by lipofuscin granules which accumulate in human cortex. Slides were mounted with Aqua-Poly/Mount medium.

Images were captured on the Leica SP8 confocal microscope. Specifically, consistent regions of interest were identified between subjects based on gyri formation, with the anterior most point of each section imaged. 11 z-stack images were taken at 0.5µm distance. The grey matter of BA9 can be characterised by 10 sub-layers containing different densities of cortical neurons and glia (Economo et al., 2008). Separate images of the upper and lower layers of BA9 were thus taken based on visual nuclei morphology and density, and distance to the cortex edge (the dome, brink, wall or valley) or the white matter. The superficial image approximately represents layer II and III (external granular layers) and IV (internal granular layer) of BA9, capturing small, medium, large and super large pyramidal cells, while the deeper image approximately captures layers V (internal pyramidal layer) to VI (spindle cell layer), which contain fewer and smaller pyramidal cells, fusiform cells and higher density of glia(von Economo, 1929). *FKBP5* long transcript probes were detected with cyanine 3 at 570nm, and the short transcript in cyanine 5 at 650nm. Optimal exposure time and image processing procedures were determined using positive controls (POL2RA for the long transcripts and PPIB for the short transcript), which were undetectable in sections hybridised with the negative control probe DapB. All images were captured using these same parameters under 40X magnification. For analyses, Fiji software (Schindelin et al., 2012) was used to merge the 11 z-stacks into one image, adjust thresholds, and automatically quantify the number of nuclei and transcripts for each probe, with one dot representing one transcript. The number of transcript dots were normalised to the number of nuclei, and the average dots for each duplicate subject was calculated. Logistic regressions, spearman partial correlations and the *nlcor* package in R were used to assess the relationship between *FKBP5* gex with age.

11. Triple-label Fluorescent Immunohistochemistry

To quantify cellular and subcellular localisation of FKBP51 protein, triple-label immunohistochemistry was performed in postmortem brain Series 3. Fresh frozen tissue blocks were cryosectioned at 50µm, mounted onto Superfrost Plus Gold slides. Sections were post-fixed with 4% PFA and antigen retrieval was performed using 10mM citric acid buffer with 0.5% Tween-20 for 10mins. Tissue was permeabilised with 0.3% Triton X-100 in phosphate buffered saline (PBS) for 5mins and blocked with 10% normal serum, 1% bovine serum albumin, with 0.3M glycine in PBS at room temperature for 1hr. Tissue was then incubated overnight at 4°C in a primary antibody solution containing rabbit anti-FKBP51 (1:300, Cell Signalling, #8245S or 1:300, Santa Cruz Biotechnology, #D-4; antibodies validated: Figure S1), neuronal marker (1:300 mouse anti-NeuN, Millipore MAB377), microglia marker (1:100, rabbit anti-TMEM119, Abcam #ab185333) and astrocyte marker (1:100, chicken anti-GFAP, Millipore AB5541). Following washing, appropriate secondary antibodies and DAPI were applied (anti-rabbit 488, anti-chicken 546, anti-mouse 647 at 1:150; DAPI at 1:5,000). Tissues were counterstained with autofluorescence eliminator reagent (Merck Millipore-2160) and cover-slipped with Aqua-Poly/Mount medium. Images were captured on the Leica SP8 confocal microscope at 40x magnification.

Series 4

12. Single-nuclei RNA sequencing

We characterised the cell-type specificity of *FKBP5* gex in BA9 with single-nucleus RNA sequencing (snRNAseq) data from Series 4 (Nagy et al., 2020). snRNAseq was performed using the 10X Genomics Chromium system (Version 2 chemistry). Data were processed with Cellranger and Seurat to identify cell-type clusters, and differential expression analysis was used for identifying genes enriched in specific major and sub-type cell clusters as previously described(Nagy et al., 2020). The FindAllMarkers function was used with the bimodal test and logfc.threshold of log(2), with other parameters set to default. *FKBP5* expression per single cell was extracted. All cells were scaled to 10,000 reads and then averaged per subject to create a pseudo cell per subject per classified cell-type in the dataset. *FKBP5* expression per cell-type was assessed for case-control differences accounting for age, PMI, RIN, pH and batch, by including these variables as covariates in linear regression modelling on transformed data to account for skewedness. The *FKBP5* aging trajectory per cell-type was assessed using spearman correlations. Note that excitatory neuron sub-clusters Ex 1, Ex 5 and Ex 9 were removed due to a large number of zero-expressors which skewed the data, and an inability to determine if these subjects were low expressors or technical dropouts.

SUPPLEMENTAL INFORMATION

Contents

A. Supplemental Methods
1. Dissection protocols, clinical and demographic details for postmortem cohorts
    a. Supplemental Table 1: Demographics of the LIBD lifetime cohort
    b. Supplemental Table 2: Demographics of the Victorian Brain Bank cohort
    c. Supplemental Table 3: Demographics from the Munich Brain Bank cohort
    d. Supplemental Table 4: Demographics from the Douglas-Bell Canada Brain Bank cohort
2. Antibody validation experiments
    a. Supplemental Table 5: FKBP51 antibodies validated in FKBP51 knock-out cells
3. Primer design for real-time quantitative PCR experiments
    a. Supplemental Table 6: RT-qPCR primer design

B. Supplemental Results
4. Supplemental Table 7: Sample sizes for genotype analyses
5. Supplemental Table 8: Functional groupings of *FKBP5* CpGs
6. Supplemental Table 9: Partial correlation of DNAm vs gex in each functional group and potentially independently functioning CpGs
7. Supplemental Table 10: Case-control differences in DNAm between *FKBP5* functional CpG groups
8. Supplemental Table 11: Partial spearman correlations of DNAm in each individual CpG/functional region with age, in the total cohort, ages 14 to 75 years
9. Supplemental Table 12: Case-control differences in *FKBP5* gex between excitatory neuron sub-clusters from Series 4 using linear regression modelling
10. Supplemental Table 13: Results of Spearman correlations assessing the relationship between *FKBP5* gex with age in each cell cluster from Series 4

C. Supplemental Figure S1
11. Figure S1: validation of FKBP51 antibodies, association of FKBP5 gene expression with age in Series 2, quantitative PCR experiment results from Series 3, and DNA methylation differences from Series 1.

D. References

A. SUPPLEMENTAL METHODS

1. Dissection protocols, clinical and demographic details for postmortem cohorts

Postmortem brain Series 1

The LIBD cohort (Series 1; Supplemental Table 1a) consisted of 252 control subjects ranging from neonate, infant, child, adolescent and adult age-groups, and 184 schizophrenia (SZ) subjects, 69 bipolar disorder (BPD) and 152 major depressive disorder (MDD) cases. Brains from Series 1 were collected at the Clinical Brain Disorders Branch (CBDB), the US National Institute of Mental Health (NIMH), the Northern Virginia and the District of Columbia Medical Examiner's Office (informed consent obtained from legal next of kin for all cases; NIMH Protocol 90-M-0142). Additional fetal, child, and adolescent brain samples were obtained through the National Institute of Child Health and Human Development Brain and Tissue Bank for Developmental Disorders (N01-HD-4-3368 and N01-HD-4_3383). Briefly, DLPFC grey matter from fetal cases was extracted using a dental drill from hemisected 1-1.5cm coronal slabs. For non-fetal cases, Brodmann area 9 and 46 were dissected from the middle frontal gyrus immediately anterior to the genu of the corpus callosum. Dissected tissues

were pulverized and stored at -80°C. Detailed information about brain tissue collection and retrieval are available elsewhere (Tao et al., 2017).

Supplemental Table 1. Demographics of the LIBD lifetime cohort

Descriptive	Group; mean (range)*			
	CTRL	**MDD**	**BD**	**SCZ**
Subjects	340	132	59	102
Age at death, yr	30.12 (14 weeks prenatal to 85)	43.7 (21-64)	43.7 (21-65)	46.0 (20-62)
Sex, male:female	228:112	79:53	32:27	69:33
PMI, h	24.79 (1-90)	36.4 (5-160)	29.5 (5-65)	39.0 (7-142)
pH	5.72 (5.9-7.1)	6.4 (5.9-7.3)	6.3 (5.9-6.9)	6.4 (5.9-7.0)
RIN	8.4 (5-10)	8.0 (5.1-9.5)	7.8 (5.0-9.3)	8.0 (5.4-9.4)
Cause of Death†, 1:2:3:4:5	2:53:186:0:37	2:20:28:79:1	2:7:11:39:0	3:15:64:20:0
Ethnicity‡ 1:2:3:4	145:177:9:9	116:11:3:2	49:5:2:3	55:42:2:3

Abbreviations: CTRL, control; MDD, major depressive disorder; BPD, bipolar disorder; SCZ, schizophrenia; PMI, postmortem interval; RIN, RNA integrity number. *Unless otherwise indicated. † 1 = Undetermined, 2 = Accident, 3 = Natural, 4 = Suicide, 5 = Homicide. ‡ 1 = Caucasian, 2 = African American, 3 = Hispanic, 4 = Asian.

Postmortem brain Series 2

The Victorian brain bank cohort (Series 2; Table 1c) consists of 20 schizophrenia, 20 major depression and 16 bipolar subjects, as well as 20 matched controls. The Diagnostic Instrument for Brain Studies was used to conduct case history reviews to reach a diagnostic consensus using the DSM-IV criteria. Regarding dissection, briefly, BA9 was isolated from the lateral surface of the frontal lobe containing the middle frontal gyrus superior to the inferior frontal sulcus. Tissue blocks were stored at -80°C until processing for downstream applications. The collection and dissection process has been previously described in detail (Scarr et al., 2018).

Supplemental Table 2: Demographics of the Victorian Brain Bank cohort, postmortem samples of dorsolateral prefrontal cortex (BA9) from the left hemisphere

Descriptive	Group; mean (range)*			
	CTRL	**MDD**	**BPD**	**SCZ**
Subjects	20	20	16	20
Age at death (years)	59.2 (32-80)	85.0 (27-87)	59.4 (31-79)	56.4 (30-82)
Sex (male:female)	11:9	11:9	8:8	11:9
Suicide (no:yes)	19:1	3:17	10:6	14:6
Brain pH	6.3 (5.9-6.7)	6.5 (5.6-6.9)	6.3 (6.0-6.5)	6.3 (5.5-6.6)
PMI (hours)	43.0 (17-72)	43.4 (11-72)	38.7 (8-63)	44.2 (20-66)
Brain weight (grams)	1354 (1140-1655)	1285 (1030-1573)	1244 (952-1630)	1337 (1110-1659)

Abbreviations: CTRL, control; MDD, major depressive disorder; BPD, bipolar disorder; SCZ, schizophrenia; PMI, postmortem interval; RIN, RNA integrity number. *Unless otherwise indicated

Postmortem brain Series 3

The Munich Neurobiobank cohort (Series 3; Supplemental Table 1b) consists of 24 control subjects with ages evenly distributed over adulthood, from 37 to 88 years of age. Clinical records were provided by relatives and general practitioners and all assessments and postmortem evaluations were conducted in accordance with the Ethics Committee of the Faculty of Medicine, University of Heidelberg, Germany. Controls had no history of alcohol or drug abuse, severe physical or psychiatric illness. Tissue blocks (~1-1.5cm^2) were dissected from the anterior-most point of the superior frontal gyrus, corresponding to BA9. Braak neuropathological examinations were staged at ≤2 for all subjects. Tissue blocks were stored at -80°C until processing for downstream applications.

Supplemental Table 3: Demographics from Munich Brain Bank, postmortem control cohort with samples from the dorsolateral prefrontal cortex (BA9)

	Group; mean (range)*
Descriptive	**CTRL**
Subjects	24
Age at death (years)	65.5 (37-88)
Sex (male:female)	13:11
Hemisphere (left:right)	11:13
PMI (hours)	32.6 (13-71)
RIN	6.1 (3.0-8.3)

Abbreviations: CTRL, control; MDD, major depressive disorder; BPD, bipolar disorder; SCZ, schizophrenia; PMI, postmortem interval; RIN, RNA integrity number. *Unless otherwise indicated

Postmortem brain Series 4

The Douglas-Bell Canada Brain Bank cohort (Series 4, Supplemental Table 4) consists of a total of 17 cases with major depressive disorder who died by suicide, and 17 matched controls. All cases were males, and samples matched by age, PMI and RIN. Cause of death was determined by the Quebec Coroner's office, and frozen grey matter from BA9 isolated by trained neuroanatomists. Psychological autopsies were performed using proxy-based interviews. Cases met criteria for MDD and died by suicide, and controls were individuals who died suddenly and did not have evidence of any axis I disorders. The study was approved by the Douglas Hospital Research Ethics Board. Written informed consent was received from the next of kin for each individual.

Supplemental Table 4. Demographics from Douglas-Bell Canada Brain Bank postmortem cohort with samples from the dorsolateral prefrontal cortex (BA9).

	Group (mean±standard deviation*)	
Descriptive	**Control**	**MDD**
Subjects	17	17
Age at death (years)	38±4.32	41.69±4.76
Sex (male:female)	17:0	17:0
Cause of death	Natural death (11), accident (6)	Suicide (17)

Brain pH	6.49±0.06	6.60±0.07
PMI (hours)	34.01±4.94	41.69±4.76
RIN	6.16	6.47

Abbreviations: MDD, major depressive disorder; PMI, postmortem interval; RIN, RNA integrity number. *Unless otherwise indicated

2. Antibody validation experiments

To validate the FKBP51 antibodies used in our study, immunoblots were performed in FKBP51 knock out (KO) cells. The KO cells were generated from the SH-SY5Y human neuroblastoma cell line using CRISPR-Cas9 (Martinelli et al.). Considering FKBP51 is lowly expressed at baseline, the synthetic glucocorticoid receptor agonist dexamethasone was also added to induced FKBP5 expression and increase visible expression of FKBP51 protein (Figure S1). Protein was extracted from cell lysates and 20ug was loaded for immunoblot analyses. FKBP51 antibodies (Supplemental Table 5) were applied (on individually run membranes) at 1:1000, and membranes were imaged according to the general methods.

Supplemental Table 5. FKBP51 antibodies validated in FKBP51 knock-out cells

Name	Type	Concentration	Number	Company
Rabbit anti-FKBP51	polyclonal	1:1000	#8245S	Cell Signaling, Danvers, MA, USA
Rabbit anti-FKBP51	polyclonal	1:1000	#A301-429A	Bethyl Laboratories, Montgomery, TX, USA
Mouse anti-FKBP51	polyclonal	1:1000	#D-4	Santa Cruz Biotechnology, Dallas, TX, USA

3. Primer design for real-time quantitative PCR experiments

Supplemental Table 6. RT-qPCR primer design

	Details		FKBP5 target	Region
1	IDT Ref	Hs.PT.58.813038 (all transcripts Exon 11-12)	**All transcripts**	Exon 11-12
	Probe	/56-FAM/CTG TTG AAT /ZEN/GCT GTG ACA AGG CCC /3IABkFQ/		
	Primer 1	ATG TGC TAC CTG AAG CTT AGA G		
	Primer 2	CCC TCC TAT ACA AGC CTT TCT C		
2	IDT Ref	Hs.PT.58.20523859 (all transcripts Exon 5-6)	**All transcripts**	Exon 5-6
	Probe	/56-FAM/AGAGATATG/ZEN/CCATTTACTGTGCAAACCAGA/3IABkFQ/		
	Primer 1	GAACCATTTGTCTTTAGTCTTGGC		
	Primer 2	CGAGGGAATTTTAGGGAGACTG		
3	IDT Ref	Hs.PT.39a.22214836 (GAPDH (NM_002046) Exon 2-3)	**GAPDH**	Exon 2-3
	Probe	/56-FAM/AAGGTCGGA/ZEN/GTCAACGGATTTGGTC/3IABkFQ/		
	Primer 1	ACATCGCTCAGACACCATG		
	Primer 2	TGTAGTTGAGGTCAATGAAGGG		
4	IDT Ref	Hs.PT.39a.22214847 (ACTB Exon 1-2)	**ACTB**	Exon 1-2
	Probe			
	Primer 1			
	Primer 2			

B. SUPPLEMENTAL RESULTS

Supplemental Table 7. Sample sizes for genotype analyses

Rs1360780, Sample size (n)		
	T carrier	CC
Control	108	64
Schizophrenia	69	45
Major Depression	78	62
Bipolar	32	28

Supplemental Table 8. Functional groupings of *FKBP5* CpGs

CpG name	chromStart	chromEnd	Position information	Group name	Sub-stratification
cg05593667	35490743	35490744	Distal TAD	distal_TAD	
cg02837122	35490787	35490788	Distal TAD		
cg18468088	35490817	35490818	Distal TAD		
cg20719122	35523699	35523700	3' downstream	downstr_conserv	
cg04192760	35523734	35523735	3' downstream		
cg07633853	35569471	35569472	Intron 5	GRE_intron5	
cg14284211	35570223	35570224	Intron 5		
cg00862770	35655763	35655764	Transcription start site	TSS	
cg00140191	35656242	35656243	Transcription start site		
cg10913456	35656589	35656590	Transcription start site		
cg16012111	35656757	35656758	Transcription start site		
cg07843056	35656847	35656848	Transcription start site		
cg01294490	35656905	35656906	Transcription start site		
cg20813374	35657180	35657181	Transcription start site		
cg00130530	35657202	35657203	Transcription start site		
cg23416081	35693572	35693573	Proximal enhancer	Prox_enhancer_total	a
cg00052684	35694245	35694246	Proximal enhancer		b
cg06937024	35695489	35695490	Proximal enhancer		Prox_enhancer_1
cg11845071	35695859	35695860	Proximal enhancer		
cg00610228	35695933	35695934	Proximal enhancer		
cg07485685	35696060	35696061	Proximal enhancer		
cg17030679	35696299	35696300	Proximal enhancer		
cg25114611	35696870	35696871	Proximal enhancer		c
cg19226017	35697184	35697185	Proximal enhancer		d
cg08915438	35697759	35697760	Proximal enhancer		e
cg07944278	35699424	35699425	Proximal enhancer		Prox_enhancer_2
cg05741161	35699498	35699499	Proximal enhancer		
cg26868354	35699951	35699952	Proximal enhancer		
cg13719443	35700381	35700382	Proximal enhancer		
cg10780318	35704148	35704149	Prox TAD	Prox_TAD	
cg01321308	35704223	35704224	Prox TAD		

Abbreviation: TAD, topologically associated domain

Supplemental Table 9. Partial correlation of DNAm vs gex in each functional group and potentially independently functioning CpG after correcting for age, sex, race, PMI and batch correction. R represents the the partial correlation coefficient between DNAm and age variables after correcting for

	all subjects		**all cases**		**control**		**schizophrenia**		**depression**		**bipolar**	
	P (nominal)	*R*	*P (nominal)*	*R*	*P (nominal)*	*R*	*P (nominal)*	*R*	*P (nominal)*	*R*	*P (nominal)*	*R*
Distal_TAD	4.66E-01	-0.03	3.40E-01	-0.05	7.21E-01	-0.03	8.76E-01	-0.01	4.22E-01	0.07	7.46E-01	0.04
downstr_conserv	**2.24E-02**	-0.10	**8.73E-04**	-0.19	1.64E-01	0.11	**4.66E-02**	-0.19	5.08E-01	0.06	7.42E-02	-0.24
GRE_intron5	1.33E-01	-0.07	9.32E-01	-0.09	3.51E-01	-0.07	1.43E-01	-0.14	5.00E-01	0.06	9.32E-01	0.01
TSS	2.05E-01	-0.06	3.92E-01	-0.05	4.79E-01	-0.05	4.21E-01	-0.08	4.54E-01	-0.06	5.94E-01	0.07
cg23416081 a	6.33E-02	-0.08	1.20E-01	-0.09	**1.61E-02**	-0.18	4.90E-01	-0.07	5.04E-01	-0.06	4.80E-01	0.10
cg00052684 b	**6.04E-03**	-0.12	**3.53E-02**	-0.12	**4.78E-02**	-0.15	2.52E-01	-0.11	7.74E-02	-0.15	2.86E-01	-0.15
Prox_enhancer_tot	**1.09E-03**	-0.15	**9.77E-03**	-0.14	**3.94E-02**	-0.16	2.91E-01	-0.10	**6.81E-03**	-0.23	7.65E-01	-0.04
Prox_enhancer_1	4.82E-01	-0.03	4.11E-01	-0.05	8.89E-01	0.01	7.98E-01	0.02	1.56E-01	-0.12	8.26E-01	-0.03
Prox_enhancer2	4.82E-01	0.03	5.21E-01	0.06	8.59E-01	-0.01	2.03E-01	0.12	**1.40E-02**	-0.08	3.35E-01	0.09
cg25114611 c	5.12E-02	-0.09	2.44E-01	-0.07	1.79E-01	-0.10	1.20E-01	-0.15	8.45E-01	-0.02	9.08E-01	-0.02
cg19226017 d	**3.57E-03**	-0.13	**7.38E-04**	-0.19	9.34E-01	0.01	**3.12E-02**	-0.20	**1.66E-03**	-0.27	7.31E-01	-0.05
cg08915438 e	3.57E-01	-0.04	9.18E-01	-0.01	2.00E-01	-0.10	7.40E-01	0.03	2.22E-01	-0.11	9.70E-01	-0.01
Prox_TAD	7.32E-01	-0.02	7.05E-01	-0.02	1.14E-01	-0.12	7.26E-01	-0.03	8.27E-01	0.02	3.90E-01	0.12

Supplemental Table 10. Case-control differences in DNAm between *FKBP5* functional CpG groups. Results of the coefficients for diagnoses derived from linear regressions are presented. Nominal and FDR corrected P values are reported. Comparisons P_{FDR}<0.05 and %max difference >1% are bolded.

	All cases vs controls				**Schizophrenia vs controls**				**Depression vs controls**				**Bipolar vs controls**			
	P_{nom}	P_{FDR}	t	% mean dif (range)	P_{nom}	P_{FDR}	t	% mean dif (range)	P_{nom}	P_{FDR}	t	% mean dif (range)	P_{nom}	P_{FDR}	t	% mean dif (range)
Distal_TAD	0.482	0.624	0.703	+0.60% (0.198-1.99)	0.594	0.644	0.553	+4.78% (0.198-0.207)	**0.005**	**0.033**	-2.853	**-5.03%** (0.198-0.187)	**0.010**	**0.043**	2.587	**+5.34%** (0.198-0.208)
downstr_conserv	0.235	0.509	-1.188	-3.03% (0.742-0.719)	0.114	0.354	-1.587	-1.26% (0.742-0.732)	**0.004**	**0.033**	-2.916	**-5.70%** (0.742-0.699)	**0.001**	**0.013**	**3.303**	**-0.41% (0.742-0.739)**
GRE_intron5	0.473	0.624	0.719	+0.58% (0.342-0.344)	0.509	0.602	0.662	-1.86% (0.342-0.366)	0.024	0.078	-2.263	+0.01% (0.342-0.342)	0.043	0.093	2.033	+6.50% (0.342-0.365)
TSS	0.538	0.636	-0.616	+0.99% (0.248-0.250)	0.239	0.444	-1.180	-0.28% (0.248-0.247)	0.809	0.919	0.242	+2.63% (0.248-0.254)	0.529	0.573	-0.630	+0.52% (0.248-0.249)
cg23416081 a	0.145	0.377	1.458	+1.96% (0.276-0.271)	0.232	0.444	1.199	+2.69% (0.276-0.269)	0.019	0.078	-2.361	-4.01% (0.276-0.265)	**0.010**	**0.043**	2.610	**+3.99%** (0.276-0.287)
cg00052684 b	0.372	0.624	-0.893	-4.52% (0.525-0.501)	0.319	0.518	-0.998	-7.24% (0.525-0.487)	0.788	0.919	0.270	+2.21% (0.525-0.513)	0.408	0.535	-0.829	-4.56% (0.525-0.501)
Prox_enhancer_tot	0.144	0.377	-1.462	+0.71% (0.297-0.295)	0.136	0.354	-1.495	+2.29% (0.297-0.291)	0.891	0.919	-0.137	+0.77% (0.297-0.300)	0.388	0.535	-0.866	+1.07% (0.297-0.294)
Prox_enhancer_1	0.440	0.624	-0.773	+0.04% (0.095-0.095)	0.477	0.602	-0.712	-1.35% (0.095-0.093)	0.912	0.919	-0.111	+1.50% (0.095-0.096)	0.986	0.986	-0.017	-0.59% (0.095-0.094)
Prox_enhancer2	0.822	0.891	0.225	+3.13% (0.156-0.161)	0.917	0.917	-0.104	+0.11% (0.156-0.156)	0.170	0.368	1.375	+6.16% (0.156-0.166)	0.417	0.535	-0.814	+2.05% (0.156-0.159)
cg25114611 c	**0.001**	**0.007**	-3.251	**-2.94%** (0.701-0.681)	**0.001**	**0.004**	-3.361	**-4.25%** (0.701-0.671)	0.683	0.919	-0.408	-1.59% (0.701-0.690)	0.019	0.052	-2.367	-3.47% (0.701-0.677)
cg19226017 d	0.944	0.944	0.071	+0.62% (0.801-0.806)	0.394	0.569	0.853	+0.01% (0.801-0.801)	0.919	0.919	-0.102	+1.95% (0.801-0.816)	0.082	0.152	-1.745	-1.21% (0.801-0.791)
cg08915438 e	0.037	0.160	-2.095	-0.61% (0.762-0.757)	**0.001**	**0.004**	-3.446	**-1.88%** (0.762-0.747)	0.042	0.109	2.040	+0.63% (0.762-0.766)	0.453	0.534	-0.751	-0.99% (0.762-0.754)
Prox_TAD	**0.000**	**0.000**	3.855	**+7.57%** (0.299-0.247)	**0.000**	**0.000**	3.847	**+7.59%** (0.299-0.247)	0.251	0.466	-1.150	+5.85% (0.299-0.243)	0.020	0.052	2.343	+11.38% (0.299-0.255)

Abbreviations: % mean dif: = % difference between means of controls vs case groups, range = mean of controls-mean of cases. Nom = nominal.

Supplemental Table 11. Partial spearman correlations (covarying for sex, race and PMI) of DNAm in each individual CpG/functional region with age, in the total cohort, ages 14 to 75 years. R values, nominal P and FDR-corrected P values are reported.

	R value	P_{NOM}	P_{FDR}
Total_gex	0.3137577	7.73E-13	1.35E-12
distal_TAD	0.4649173	4.50E-28	1.05E-27
downstr_conserv	-0.0426742	3.42E-01	3.46E-01
GRE_intron5	-0.4587783	2.73E-27	5.45E-27
TSS	-0.0489672	2.75E-01	3.21E-01
Prox_enhancer_tot	-0.7883986	9.92E-107	6.94E-106
Prox_enhancer_1	-0.1017775	2.31E-02	2.94E-02
Prox_enhancer2	-0.1240663	5.56E-03	7.79E-03
Prox_TAD	-0.0423328	3.46E-01	3.46E-01
cg23416081 a	-0.7050586	4.68E-76	2.19E-75
cg00052684 b	-0.2127109	1.67E-06	2.60E-06
cg25114611 c	-0.5067513	7.61E-34	2.13E-33
cg19226017 d	-0.5995894	6.17E-50	2.16E-49
cg08915438 e	-0.8230384	6.16E-124	8.62E-123

Supplemental Table 12. Case-control differences in *FKBP5* gex between excitatory neuron sub-clusters from Series 4 using linear regression modelling. Results of the coefficients for diagnoses derived from the linear regressions (*lm* function) are presented. Nominal and FDR-corrected P values for multiple comparisons across cell types are reported.

Major/sub-cluster name	**Cortical layer(s)**	**t-value**	**P_{nom}**	**P_{FDR}**
Astrocytes	-	1.079	0.29058	0.5749333
Endothelium	-	0.328	0.744114	0.744114
Inhibitory	-	0.695	0.4928	0.5749333
Microglia	-	1.335	0.18717	0.5749333
Oligodendrocytes	-	-0.731	0.471	0.5749333
Oligodendrocyte progenitor cell	-	0.766	0.4445	0.5749333
Excitatory	-	-1.776	0.0267	0.1869
Ex 2	5	0.066	0.948	0.9480000
Ex 3	4-5	0.478	0.638	0.7443333
Ex 4	6	-0.687	0.4990	0.6986000
Ex 6	4-6	0.729	0.4723	0.6986000
Ex 7	4-6	-0.978	0.33673	0.6986000
Ex 8	5-6	-1.596	0.1226	0.4291000
Ex 10	2-4	**-2.190**	**0.0364**	0.2548000

Supplemental Table 13. Results of Spearman correlations assessing the relationship between *FKBP5* gex with age in each cell cluster from Series 4. Nominal and FDR-corrected P values are reported.

Major/sub-cluster name	**Cortical layer(s)**	**R-value**	**P_{nom}**	**P_{FDR}**
Oligodendrocytes	-	**0.4011025**	**0.0187**	**0.0479**
Astrocytes	-	**0.4015578**	**0.0205**	**0.0479**
Oligodendrocyte progenitor cell	-	0.3309074	0.0559	0.0979
Inhibitory neurons	-	0.2962397	0.0889	0.1245
Endothelial cells	-	0.1257452	0.4786	0.5584
Microglia	-	0.09823437	0.5927	0.5927
Excitatory neurons	-	**0.6638643**	**1.87E-05**	**1.31E-04**
Ex 2	5	0.1197	0.5138	0.7193
Ex 3	4-5	0.3377615	0.0849	0.1827
Ex 4	6	0.3023	0.1044	0.1827
Ex 6	4-6	0.3122614	0.0722	0.1827
Ex 7	4-6	0.06969655	0.6953	0.7267
Ex 8	5-6	0.6322	0.7267	0.7267
Ex 10	**2-4**	**0.69978**	**4.11E-06**	**2.88E-05**

C. Supplemental Figure

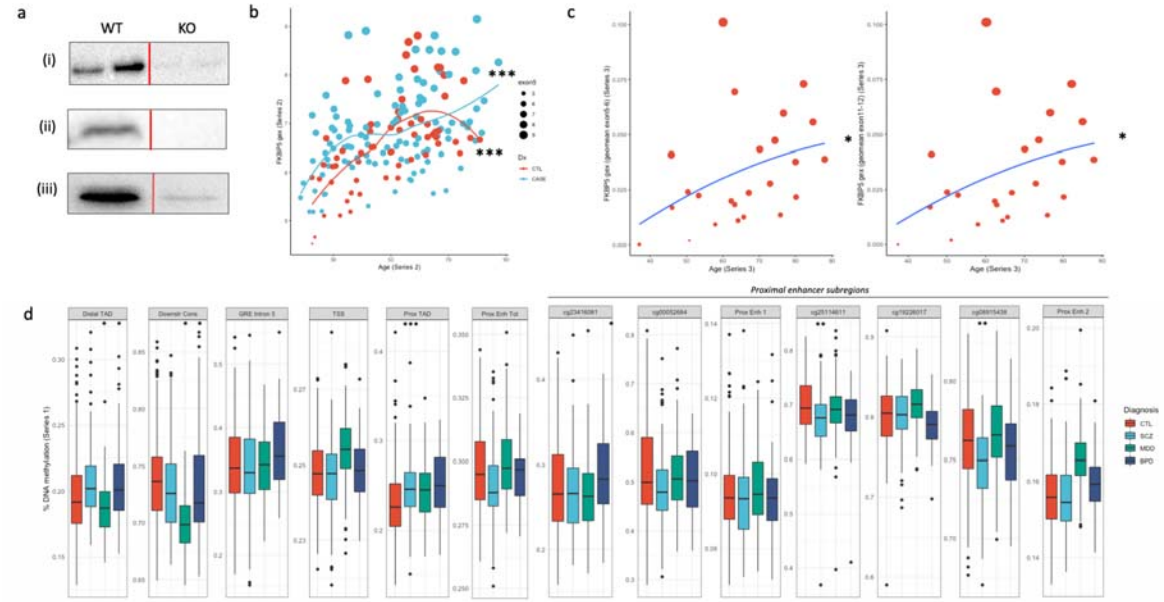

Figure S1. (a) Validation of FKBP51 antibodies in *FKBP5* knock-out HELA cells using immunoblot. All FKBP51 antibodies ([i] Cell Signalling #8245S, [ii] Bethyl #A301-429A, [iii] Santa Cruz #D-4) showed specific expression in wildtype (WT) cells but not *FKBP5* knock-out (KO) cells, indicating their specificity. **(b)** Association of *FKBP5* gene expression with age in Series 2. *FKBP5* was positively and significantly associated with age in both cases and controls, with heightened expression at older ages in cases. **(c)** Results of quantitative PCR experiments assessing the correlation between *FKBP5* expression with age in Series 3. *FKBP5* was significantly associated with age with two independent probes targeting all transcripts either at *FKBP5* exon 5-6 or 11-12. **(d)** DNAm differences across the different *FKBP5* CpGs (individual or grouped, as per Supplemental Table 8) for controls, schizophrenia, major depression and bipolar disorder subjects. *Abbreviations*: CTL, control, distal_TAD, distal topologically associated domain; DNAm, DNA methylation; Downstr_Cons, downstream conserved region; gex, gene expression; MDD, major depressive disorder; GRE, glucocorticoid response element; SCZ, schizophrenia; TSS, transcription start site; Prox Enh Tot, total DNAm across the total proximal enhancer region; Prox_Enh_1/2, DNAm levels in subsets of proximal enhancer region (detailed in Supplemental Table 8); Prox_TAD, proximal topologically associated domain. Series refer to the cohorts used in each analyses, as detailed in Table 1. Asterix indicate significance levels: *P<0.05, ***P<0.001.

REFERENCES

Anderzhanova, E., Hafner, K., Genewsky, A.J., Soliman, A., Pöhlmann, M.L., Schmidt, M.V., Blum, R., Wotjak, C.T., and Gassen, N.C. (2020). The stress susceptibility factor FKBP51 controls S-ketamine-evoked release of mBDNF in the prefrontal cortex of mice. Neurobiol Stress 13, 100239.

Arnsten, A.F.T. (2009). Stress signalling pathways that impair prefrontal cortex structure and function. Nature Reviews Neuroscience 10, 410-422.

Aryee, M.J., Jaffe, A.E., Corrada-Bravo, H., Ladd-Acosta, C., Feinberg, A.P., Hansen, K.D., and Irizarry, R.A. (2014). Minfi: a flexible and comprehensive Bioconductor package for the analysis of Infinium DNA methylation microarrays. In Bioinformatics, pp. 1363-1369.

Barsegyan, A., Mackenzie, S.M., Kurose, B.D., McGaugh, J.L., and Roozendaal, B. (2010). Glucocorticoids in the prefrontal cortex enhance memory consolidation and impair working memory by a common neural mechanism. Proc Natl Acad Sci U S A 107, 16655-16660.

Baughman, G., Wiederrecht, G.J., Campbell, N.F., Martin, M.M., and Bourgeois, S. (1995). FKBP51, a novel T-cell-specific immunophilin capable of calcineurin inhibition. Molecular and cellular biology 15, 4395-4402.

Benjamini, Y., and Hochberg, Y. (1995). Controlling the False Discovery Rate: A Practical and Powerful Approach to Multiple Testing. Journal of the Royal Statistical Society Series B (Methodological) 57, 289-300.

Blair, L.J., Criado-Marrero, M., Zheng, D., Wang, X., Kamath, S., Nordhues, B.A., Weeber, E.J., and Dickey, C.A. (2019). The Disease-Associated Chaperone FKBP51 Impairs Cognitive Function by Accelerating AMPA Receptor Recycling. eNeuro 6, ENEURO.0242-0218.2019.

Blair, L.J., Nordhues, B.A., Hill, S.E., Scaglione, K.M., O'Leary, J.C., 3rd, Fontaine, S.N., Breydo, L., Zhang, B., Li, P., Wang, L., *et al.* (2013). Accelerated neurodegeneration through chaperone-mediated oligomerization of tau. The Journal of clinical investigation 123, 4158-4169.

Bowman, A., and Azzalini, A. (1997). Applied smoothing techniques for data analysis: the kernel approach with S-Plus illustrations.

Economo, C.v., Koskinas, G., and Triarhou, L. (2008). Atlas of cytoarchitectonics of the adult human cerebral cortex, Illustrated edn (Basel, Switzerland: Karger).

Fabian, A.-K., März, A., Neimanis, S., Biondi, R.M., Kozany, C., and Hausch, F. (2013). InterAKTions with FKBPs - Mutational and Pharmacological Exploration. PLOS ONE 8, e57508.

Gaali, S., Kirschner, A., Cuboni, S., Hartmann, J., Kozany, C., Balsevich, G., Namendorf, C., Fernandez-Vizarra, P., Sippel, C., Zannas, A.S., *et al.* (2015). Selective inhibitors of the FK506-binding protein 51 by induced fit. Nature chemical biology 11, 33-37.

Gassen, N.C., Fries, G.R., Zannas, A.S., Hartmann, J., Zschocke, J., Hafner, K., Carrillo-Roa, T., Steinbacher, J., Preißinger, S.N., Hoeijmakers, L., *et al.* (2015). Chaperoning epigenetics: FKBP51 decreases the activity of DNMT1 and mediates epigenetic effects of the antidepressant paroxetine. Sci Signal 8, ra119-ra119.

Gassen, N.C., Hartmann, J., Zannas, A.S., Kretzschmar, A., Zschocke, J., Maccarrone, G., Hafner, K., Zellner, A., Kollmannsberger, L.K., Wagner, K.V., *et al.* (2016a). FKBP51 inhibits GSK3β and augments the effects of distinct psychotropic medications. Mol Psychiatry 21, 277-289.

Gassen, N.C., Hartmann, J., Zannas, A.S., Kretzschmar, A., Zschocke, J., Maccarrone, G., Hafner, K., Zellner, A., Kollmannsberger, L.K., Wagner, K.V., and others (2016b). FKBP51 inhibits GSK3β and augments the effects of distinct psychotropic medications. Molecular psychiatry 21, 277-289.

Gassen, N.C., Hartmann, J., Zschocke, J., Stepan, J., Hafner, K., Zellner, A., Kirmeier, T., Kollmannsberger, L., Wagner, K.V., Dedic, N., *et al.* (2014). Association of FKBP51 with priming of autophagy pathways and mediation of antidepressant treatment response: evidence in cells, mice, and humans. PLoS Med 11, e1001755.

Habib, N., Avraham-Davidi, I., Basu, A., Burks, T., Shekhar, K., Hofree, M., Choudhury, S.R., Aguet, F., Gelfand, E., Ardlie, K., *et al.* (2017). Massively parallel single-nucleus RNA-seq with DroNc-seq. Nat Methods 14, 955-958.

Hartmann, J., Wagner, K.V., Gaali, S., Kirschner, A., Kozany, C., Rühter, G., Dedic, N., Häusl, A.S., Hoeijmakers, L., Westerholz, S., *et al.* (2015). Pharmacological Inhibition of the Psychiatric Risk Factor FKBP51 Has Anxiolytic Properties.

Ising, M., Maccarrone, G., Brückl, T., Scheuer, S., Hennings, J., Holsboer, F., Turck, C.W., Uhr, M., and Lucae, S. (2019). FKBP5 Gene Expression Predicts Antidepressant Treatment Outcome in Depression. Int J Mol Sci 20.

Jaffe, A.E., Gao, Y., Deep-Soboslay, A., Tao, R., Hyde, T.M., Weinberger, D.R., and Kleinman, J.E. (2016). Mapping DNA methylation across development, genotype and schizophrenia in the human frontal cortex. Nature Neuroscience 19, 40-47.

Jaffe, A.E., Tao, R., Norris, A.L., Kealhofer, M., Nellore, A., Shin, J.H., Kim, D., Jia, Y., Hyde, T.M., Kleinman, J.E., *et al.* (2017). qSVA framework for RNA quality correction in differential expression analysis. Proc Natl Acad Sci U S A 114, 7130-7135.

Kaul, D., Schwab, S., Mechawar, N., and Matosin, N. (2021). How Stress Physically Re-shapes the Brain: Impact on Brain Cell Shapes, Numbers and Connections in Psychiatric Disorders. Neurosci Biobehav Rev in press.

Kendler, K.S., Karkowski, L.M., and Prescott, C.A. (1999). Causal relationship between stressful life events and the onset of major depression. The American Journal of Psychiatry 156, 837-841.

Kendler, K.S., Myers, J.M., and Keyes, C.L.M. (2011). The Relationship Between the Genetic and Environmental Influences on Common Externalizing Psychopathology and Mental Wellbeing. Twin Res Hum Genet 14, 516-523.

Klengel, T., and Binder, E.B. (2013). Allele-specific epigenetic modification: a molecular mechanism for gene-environment interactions in stress-related psychiatric disorders? Epigenomics 5, 109-112.

Klengel, T., and Binder, E.B. (2015). FKBP5 allele-specific epigenetic modification in gene by environment interaction. Neuropsychopharmacology 40, 244-246.

Klengel, T., Mehta, D., Anacker, C., Rex-Haffner, M., Pruessner, J.C., Pariante, C.M., Pace, T.W.W., Mercer, K.B., Mayberg, H.S., and Bradley, B. (2013). Allele-specific FKBP5 DNA demethylation mediates gene-childhood trauma interactions. Nature neuroscience 16, 33-41.

Kraft, P., and Aschard, H. (2015). Finding the missing gene-environment interactions. Eur J Epidemiol 30, 353-355.

Lake, B.B., Ai, R., Kaeser, G.E., Salathia, N.S., Yung, Y.C., Liu, R., Wildberg, A., Gao, D., Fung, H.L., Chen, S., *et al.* (2016). Neuronal subtypes and diversity revealed by single-nucleus RNA sequencing of the human brain. Science 352, 1586-1590.

Lake, B.B., Chen, S., Sos, B.C., Fan, J., Kaeser, G.E., Yung, Y.C., Duong, T.E., Gao, D., Chun, J., Kharchenko, P.V., and Zhang, K. (2018). Integrative single-cell analysis of transcriptional and epigenetic states in the human adult brain. Nat Biotechnol 36, 70-80.

Liao, Y., Smyth, G.K., and Shi, W. (2013). featureCounts: an efficient general purpose program for assigning sequence reads to genomic features. Bioinformatics 30, 923-930.

Matosin, N., Fernandez-Enright, F., Fung, S.J., Lum, J.S., Engel, M., Andrews, J.L., Huang, X.F., Weickert, C.S., and Newell, K.A. (2015). Alterations of mGluR5 and its endogenous regulators Norbin, Tamalin and Preso1 in schizophrenia: towards a model of mGluR5 dysregulation. Acta Neuropathol 130, 119-129.

Matosin, N., Halldorsdottir, T., and Binder, E.B. (2018). Understanding the Molecular Mechanisms Underpinning Gene by Environment Interactions in Psychiatric Disorders: The FKBP5 Model. Biol Psychiatry 83, 821-830.

Matthias Weiwad, Frank Edlich, Susann Kilka, Frank Erdmann, Franziska Jarczowski, Madlen Dorn, Marie-Christine Moutty, a., and Fischer*, G. (2006). Comparative Analysis of Calcineurin Inhibition by Complexes of Immunosuppressive Drugs with Human FK506 Binding Proteins†.

McTeague, L.M., Goodkind, M.S., and Etkin, A. (2016). Transdiagnostic impairment of cognitive control in mental illness. J Psychiatr Res 83, 37-46.

Menke, A., Klengel, T., Rubel, J., Brückl, T., Pfister, H., Lucae, S., Uhr, M., Holsboer, F., and Binder, E.B. (2013). Genetic variation in FKBP5 associated with the extent of stress hormone dysregulation in major depression. Genes Brain Behav 12, 289-296.

Moore, L.D., Le, T., and Fan, G. (2013). DNA methylation and its basic function. Neuropsychopharmacology 38, 23-38.

Myers, B., McKlveen, J.M., and Herman, J.P. (2014). Glucocorticoid actions on synapses, circuits, and behavior: implications for the energetics of stress. Front Neuroendocrinol 35, 180-196.

Nagy, C., Maitra, M., Tanti, A., Suderman, M., Théroux, J.-F., Davoli, M.A., Perlman, K., Yerko, V., Wang, Y.C., Tripathy, S.J., *et al.* (2020). Single-nucleus transcriptomics of the prefrontal cortex in major depressive disorder implicates oligodendrocyte precursor cells and excitatory neurons. Nature Neuroscience 23, 771-781.

Paakinaho, V., Makkonen, H., Jaaskelainen, T., and Palvimo, J.J. (2010). Glucocorticoid receptor activates poised FKBP51 locus through long-distance interactions. Molecular endocrinology (Baltimore, Md) 24, 511-525.

Provençal, N., Arloth, J., Cattaneo, A., Anacker, C., Cattane, N., Wiechmann, T., Röh, S., Ködel, M., Klengel, T., Czamara, D., *et al.* (2020). Glucocorticoid exposure during hippocampal neurogenesis primes future stress response by inducing changes in DNA methylation. Proc Natl Acad Sci U S A 117, 23280-23285.

Qiu, B., Xu, Y., Wang, J., Liu, M., Dou, L., Deng, R., Wang, C., Williams, K.E., Stewart, R.B., Xie, Z., *et al.* (2019). Loss of FKBP5 Affects Neuron Synaptic Plasticity: An Electrophysiology Insight. Neuroscience 402, 23-36.

Ranjan, C., and Najari Sisi, V. (2019). nlcor: Nonlinear Correlation.

Rein, T. (2016). FK506 binding protein 51 integrates pathways of adaptation: FKBP51 shapes the reactivity to environmental change. Bioessays 38, 894-902.

Scarr, E., Udawela, M., Thomas, E.A., and Dean, B. (2018). Changed gene expression in subjects with schizophrenia and low cortical muscarinic M1 receptors predicts disrupted upstream pathways interacting with that receptor. Mol Psychiatry 23, 295-303.

Schindelin, J., Arganda-Carreras, I., Frise, E., Kaynig, V., Longair, M., Pietzsch, T., Preibisch, S., Rueden, C., Saalfeld, S., Schmid, B., *et al.* (2012). Fiji: an open-source platform for biological-image analysis. Nat Methods 9, 676-682.

Schmidt, U., Buell, D.R., Ionescu, I.A., Gassen, N.C., Holsboer, F., Cox, M.B., Novak, B., Huber, C., Hartmann, J., Schmidt, M.V., *et al.* (2015). A role for synapsin in FKBP51 modulation of stress responsiveness: Convergent evidence from animal and human studies. Psychoneuroendocrinology 52, 43-58.

Tao, R., Davis, K.N., Li, C., Shin, J.H., Gao, Y., Jaffe, A.E., Gondre-Lewis, M.C., Weinberger, D.R., Kleinman, J.E., and Hyde, T.M. (2017). GAD1 alternative transcripts and DNA methylation in human prefrontal cortex and hippocampus in brain development, schizophrenia. Mol Psychiatry.

Visscher, P.M., Wray, N.R., Zhang, Q., Sklar, P., McCarthy, M.I., Brown, M.A., and Yang, J. (2017). 10 Years of GWAS Discovery: Biology, Function, and Translation. Am J Hum Genet 101, 5-22.

von Economo, C. (1929). The Cytoarchitectonics of the Human Cerebral Cortex. J Anat 63, 389.

Weickert, C.S., Webster, M.J., Boerrigter, D., and Sinclair, D. (2015). FKBP5 mRNA Increases after adolescence in human DLPFC. Biological Psychiatry.

Wiechmann, T., Röh, S., Sauer, S., Czamara, D., Arloth, J., Ködel, M., Beintner, M., Knop, L., Menke, A., Binder, E.B., and Provençal, N. (2019). Identification of dynamic glucocorticoid-induced methylation changes at the FKBP5 locus. Clinical Epigenetics 11, 83.

Young, K.A., Thompson, P.M., Cruz, D.A., Williamson, D.E., and Selemon, L.D. (2015). BA11 FKBP5 expression levels correlate with dendritic spine density in postmortem PTSD and controls. Neurobiology of stress 2, 67-72.

Young, S.G., and Bowman, A.W. (1995). Non-Parametric Analysis of Covariance. Biometrics 51, 920-931.

Zannas, A.S., Jia, M., Hafner, K., Baumert, J., Wiechmann, T., Pape, J.C., Arloth, J., Kodel, M., Martinelli, S., Roitman, M., *et al.* (2019). Epigenetic upregulation of FKBP5 by aging and stress contributes to NF-kappaB-driven inflammation and cardiovascular risk. Proc Natl Acad Sci U S A 116, 11370-11379.

Zannas, A.S., Wiechmann, T., Gassen, N.C., and Binder, E.B. (2016). Gene–Stress–Epigenetic Regulation of FKBP5: Clinical and Translational Implications. Neuropsychopharmacology 41, 261-274.

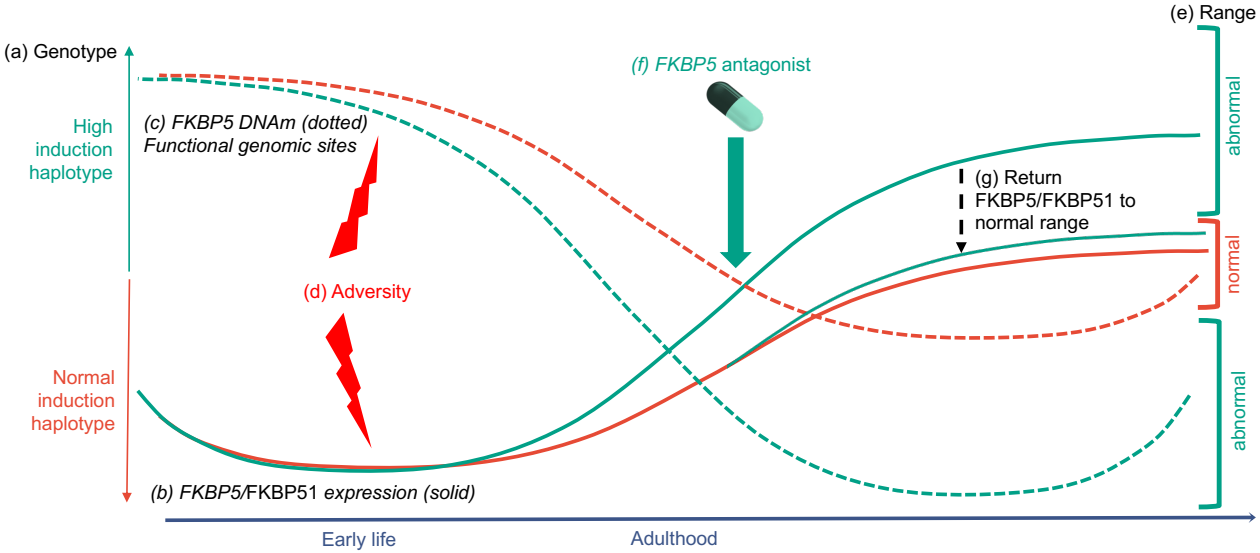
(e) Range
(a) Genotype
(f) FKBP5 antagonist
High induction haplotype
(c) FKBP5 DNAm (dotted)
Functional genomic sites
(g) Return FKBP5/FKBP51 to normal range
abnormal
normal
abnormal
(d) Adversity
Normal induction haplotype
(b) FKBP5/FKBP51 expression (solid)
Early life
Adulthood

Figure 1

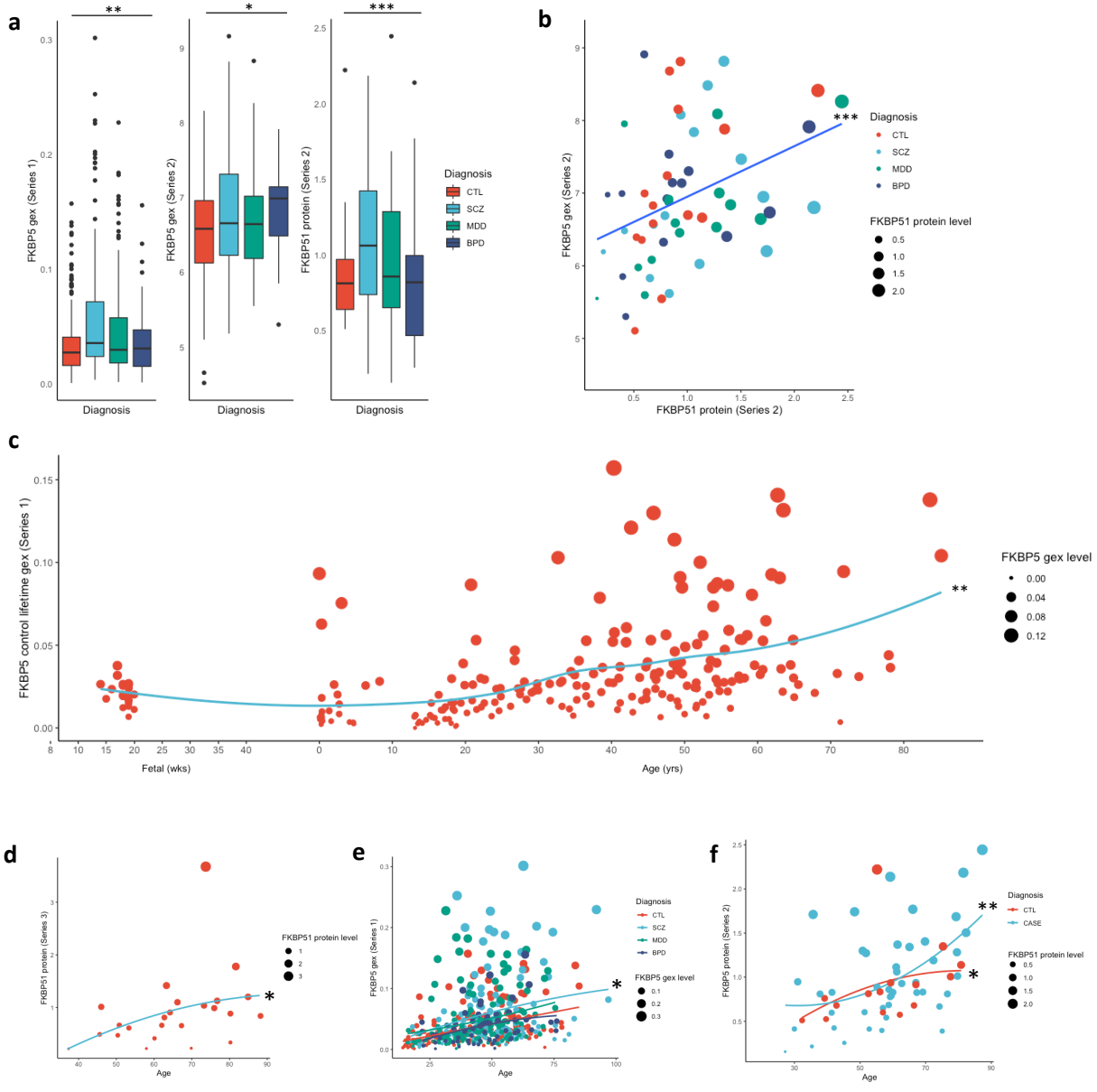
a
b
c
d
e
f
FKBP5 gex (Series 1)
FKBP5 gex (Series 2)
FKBP51 protein (Series 2)
Diagnosis
CTL
SCZ
MDD
BPD
FKBP51 protein level
FKBP5 control lifetime gex (Series 1)
Fetal (wks)
Age (yrs)
FKBP5 gex level
FKBP51 protein (Series 3)
Age
CASE

Figure 2

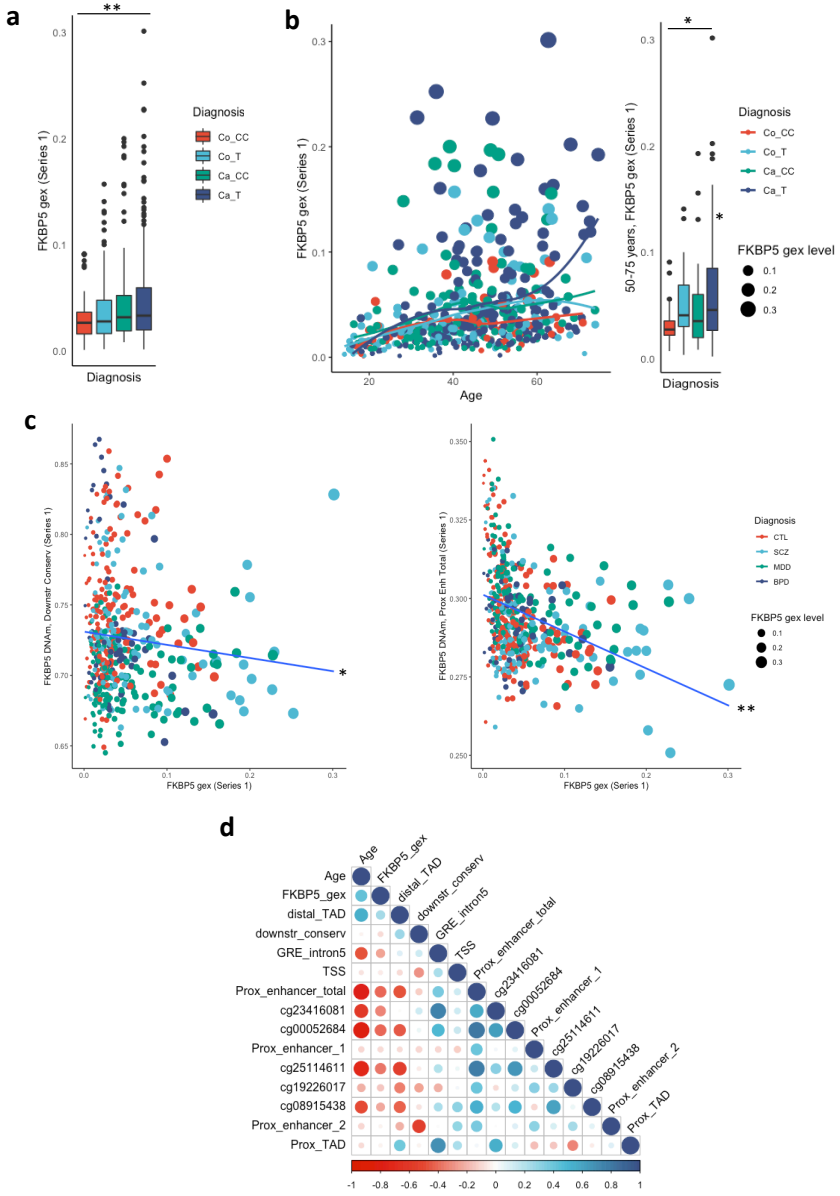
a
b
c
d
FKBP5 gex (Series 1)
Diagnosis
Co_CC
Co_T
Ca_CC
Ca_T
Age
50-75 years, FKBP5 gex (Series 1)
FKBP5 gex level
FKBP5 DNAm, Downstr Conserv (Series 1)
FKBP5 DNAm, Prox Enh Total (Series 1)
CTL
SCZ
MDD
BPD
Prox_enhancer_total
cg23416081
cg00052684
Prox_enhancer_1
cg25114611
cg19226017
cg08915438
Prox_enhancer_2
Prox_TAD
distal_TAD
downstr_conserv
GRE_intron5
TSS

Figure 3

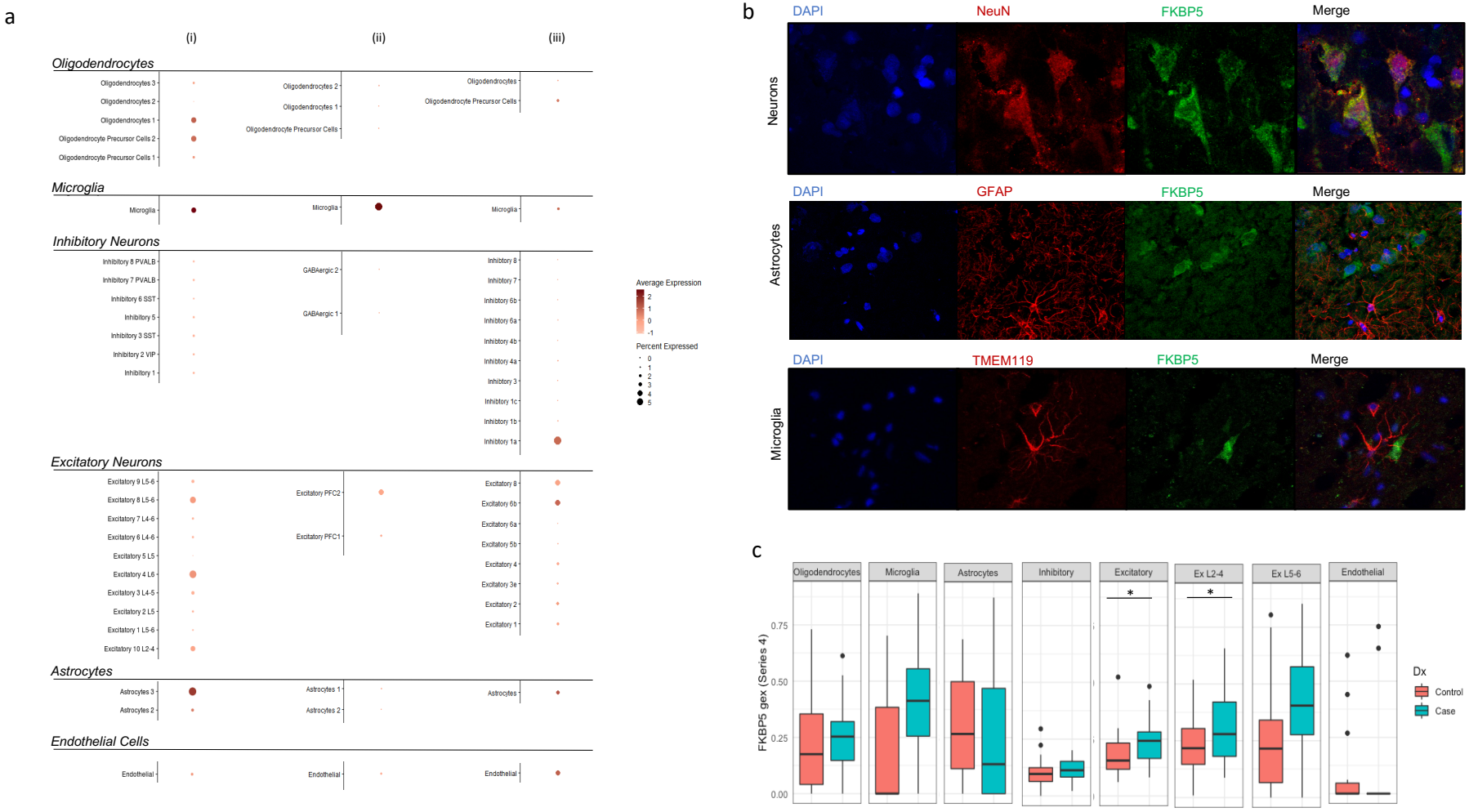
a
(i)
(ii)
(iii)
Oligodendrocytes
Oligodendrocytes 3
Oligodendrocytes 2
Oligodendrocytes 1
Oligodendrocyte Precursor Cells 2
Oligodendrocyte Precursor Cells 1
Oligodendrocytes 2
Oligodendrocytes 1
Oligodendrocyte Precursor Cells
Oligodendrocytes
Oligodendrocyte Precursor Cells
Microglia
Microglia
Microglia
Microglia
Inhibitory Neurons
Inhibitory 8 PVALB
Inhibitory 7 PVALB
Inhibitory 6 SST
Inhibitory 5
Inhibitory 3 SST
Inhibitory 2 VIP
Inhibitory 1
GABAergic 2
GABAergic 1
Inhibitory 8
Inhibitory 7
Inhibitory 6b
Inhibitory 6a
Inhibitory 4b
Inhibitory 4a
Inhibitory 3
Inhibitory 1c
Inhibitory 1b
Inhibitory 1a
Excitatory Neurons
Excitatory 9 L5-6
Excitatory 8 L5-6
Excitatory 7 L4-6
Excitatory 6 L4-6
Excitatory 5 L5
Excitatory 4 L6
Excitatory 3 L4-5
Excitatory 2 L5
Excitatory 1 L5-6
Excitatory 10 L2-4
Excitatory PFC2
Excitatory PFC1
Excitatory 8
Excitatory 6b
Excitatory 6a
Excitatory 5b
Excitatory 4
Excitatory 3e
Excitatory 2
Excitatory 1
Astrocytes
Astrocytes 3
Astrocytes 2
Astrocytes 1
Astrocytes 2
Astrocytes
Endothelial Cells
Endothelial
Endothelial
Endothelial
Average Expression
2
1
0
-1
Percent Expressed
0
1
2
3
4
5
b
DAPI
NeuN
FKBP5
Merge
Neurons
DAPI
GFAP
FKBP5
Merge
Astrocytes
DAPI
TMEM119
FKBP5
Merge
Microglia
c
Oligodendrocytes
Microglia
Astrocytes
Inhibitory
Excitatory
Ex L2-4
Ex L5-6
Endothelial
FKBP5 gex (Series 4)
0.75
0.50
0.25
0.00
*
*
Dx
Control
Case

Figure 4

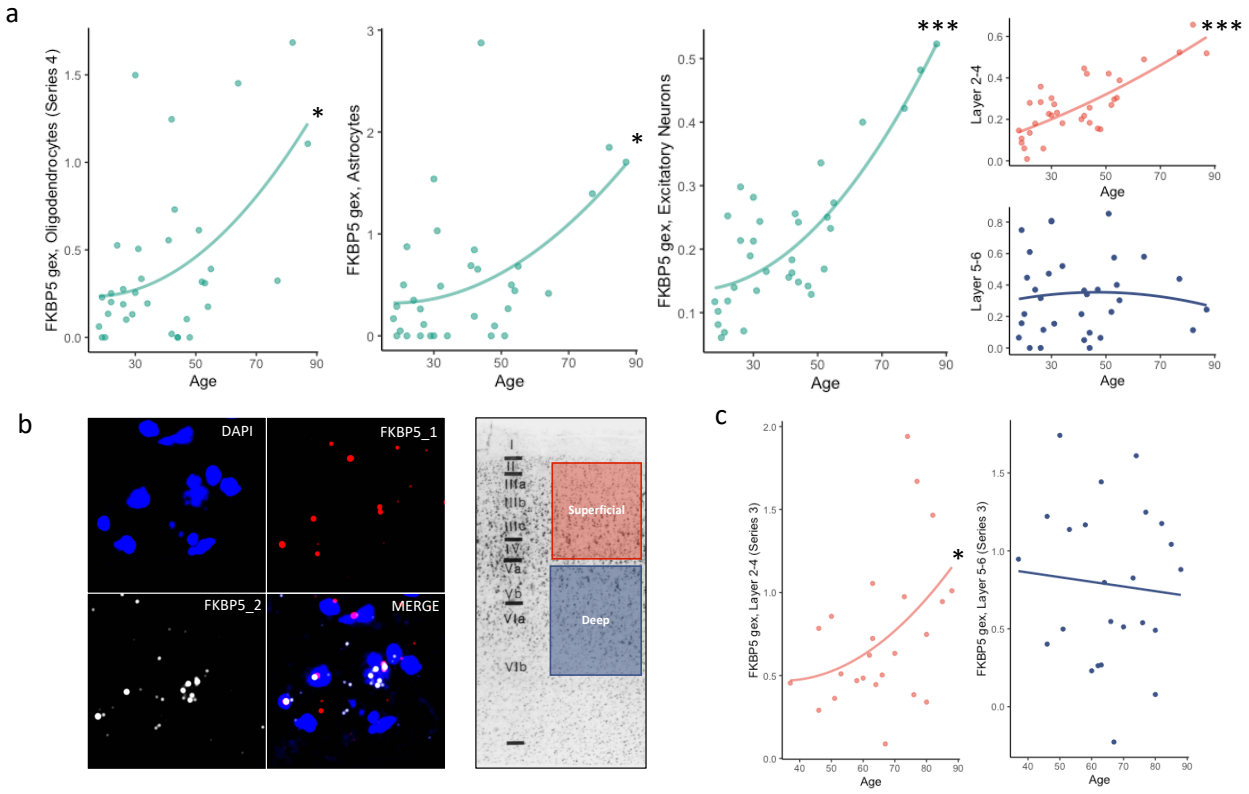
a
FKBP5 gex, Oligodendrocytes (Series 4)
FKBP5 gex, Astrocytes
FKBP5 gex, Excitatory Neurons
Layer 2-4
Layer 5-6
Age
*
***
b
DAPI
FKBP5_1
FKBP5_2
MERGE
Superficial
Deep
c
FKBP5 gex, Layer 2-4 (Series 3)
FKBP5 gex, Layer 5-6 (Series 3)

Figure 5

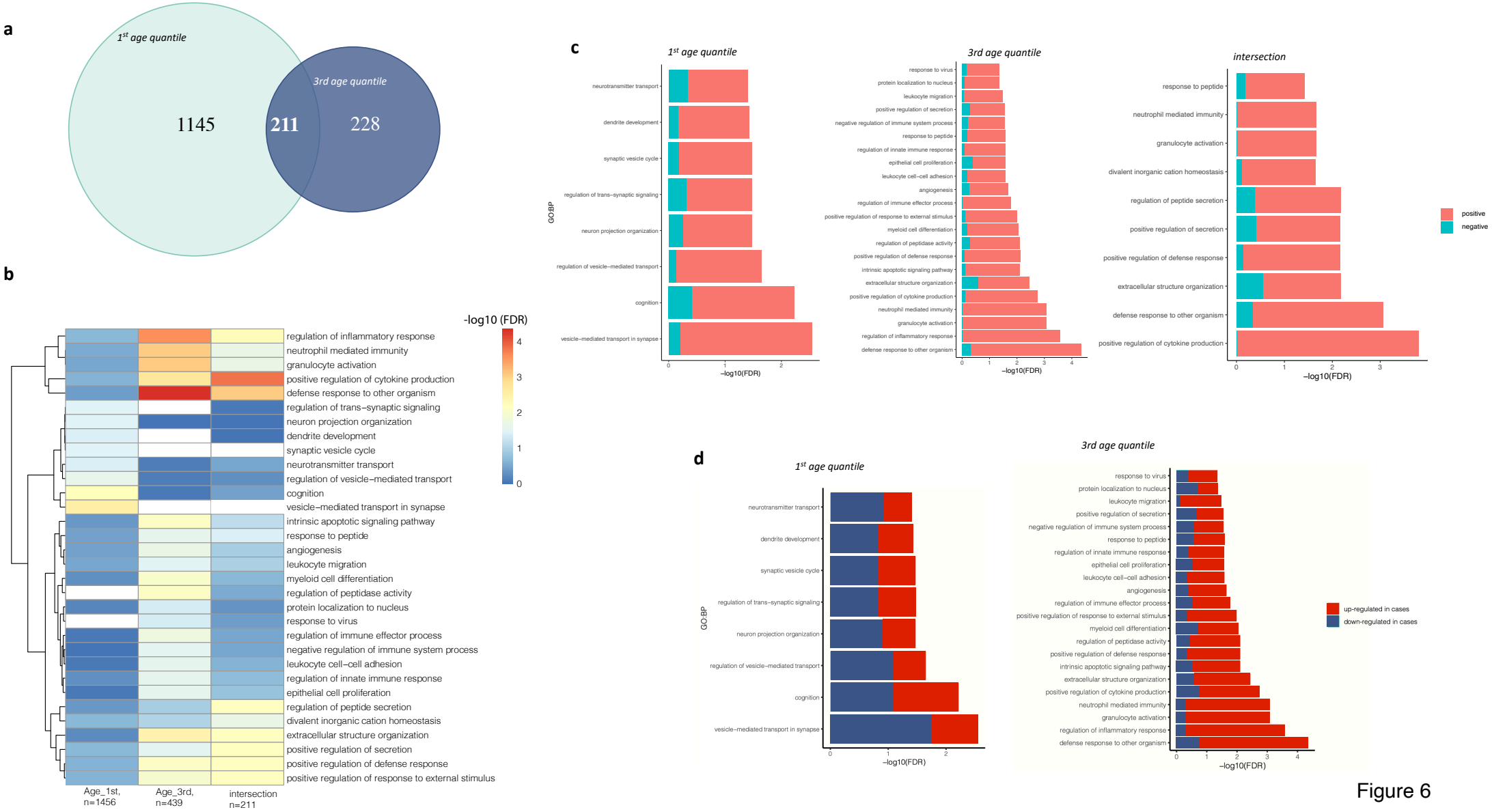
a
1st age quantile
3rd age quantile
1145
211
228
b
-log10 (FDR)
4
3
2
1
0
regulation of inflammatory response
neutrophil mediated immunity
granulocyte activation
positive regulation of cytokine production
defense response to other organism
regulation of trans−synaptic signaling
neuron projection organization
dendrite development
synaptic vesicle cycle
neurotransmitter transport
regulation of vesicle−mediated transport
cognition
vesicle−mediated transport in synapse
intrinsic apoptotic signaling pathway
response to peptide
angiogenesis
leukocyte migration
myeloid cell differentiation
regulation of peptidase activity
protein localization to nucleus
response to virus
regulation of immune effector process
negative regulation of immune system process
leukocyte cell−cell adhesion
regulation of innate immune response
epithelial cell proliferation
regulation of peptide secretion
divalent inorganic cation homeostasis
extracellular structure organization
positive regulation of secretion
positive regulation of defense response
positive regulation of response to external stimulus
Age_1st, n=1456
Age_3rd, n=439
intersection n=211
c
1st age quantile
3rd age quantile
intersection
GOBP
−log10(FDR)
positive
negative
d
1st age quantile
3rd age quantile
GOBP
−log10(FDR)
up-regulated in cases
down-regulated in cases

Figure 6

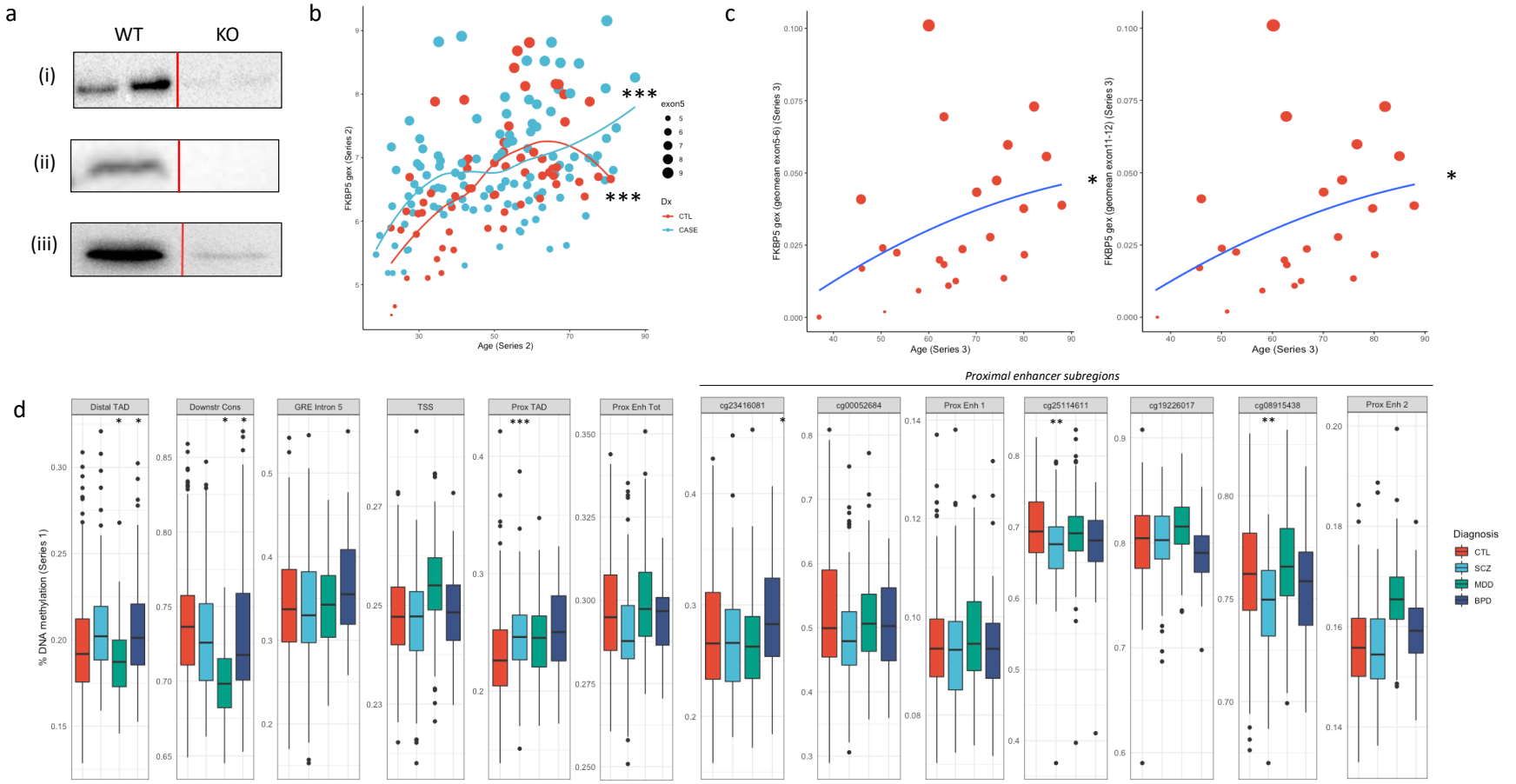

Supp Figure 1